FAKULTA ELEKTROTECHNICKÁ
FACULTY OF ELECTRICAL ENGINEERING
Technická 2
166 27 Praha 6

DECLARATION

I, the undersigned

Student's surname, given name(s): Farzaliyev Ramil
Personal number: 481621
Programme name: Electrical Engineering and Computer Science

declare that I have elaborated the bachelor's thesis entitled

Application potential of NIR to IR optical centers in diamond

independently, and have cited all information sources used in accordance with the Methodological Instruction on the Observance of Ethical Principles in the Preparation of University Theses and with the Framework Rules for the Use of Artificial Intelligence at CTU for Academic and Pedagogical Purposes in Bachelor's and Continuing Master's Programmes.

I declare that I did not use any artificial intelligence tools during the preparation and writing of my thesis. I am aware of the consequences if manifestly undeclared use of such tools is determined in the elaboration of any part of my thesis.

In Prague on 20.05.2025

Ramil Farzaliyev
.....
student's signature

BACHELOR‘S THESIS ASSIGNMENT

I. Personal and study details

Student's name: **Farzaliyev Ramil** Personal ID number: **481621**
Faculty / Institute: **Faculty of Electrical Engineering**
Department / Institute: **Department of Physics**
Study program: **Electrical Engineering and Computer Science**

II. Bachelor’s thesis details

Bachelor’s thesis title in English:
Application potential of NIR to IR optical centers in diamond

Bachelor’s thesis title in Czech:
Aplikační potenciál NIR to IR optických center v diamantu

Name and workplace of bachelor’s thesis supervisor:
Ing. Štěpán Potocký, Ph.D. Fyzikální ústav AV ČR, v.v.i.

Name and workplace of second bachelor’s thesis supervisor or consultant:

Date of bachelor’s thesis assignment: **17.02.2025** Deadline for bachelor thesis submission: **23.05.2025**

Assignment valid until: **14.02.2027**

Head of department’s signature

Vice-dean´s signature on behalf of the Dean

III. Assignment receipt

The student acknowledges that the bachelor's thesis is an individual work.
The student must produce his thesis without the assistance of others, with the exception of provided consultations.
Within the bachelor's thesis, the author must state the names of consultants and include a list of references.

Date of assignment receipt	Student's signature
	Farzaliyev Ramil

© ČVUT v Praze, Design: ČVUT v Praze, VIC

BACHELOR'S THESIS ASSIGNMENT

I. Personal and study details

Student's name: **Farzaliyev Ramil** Personal ID number: **481621**
Faculty / Institute: **Faculty of Electrical Engineering**
Department / Institute: **Department of Physics**
Study program: **Electrical Engineering and Computer Science**

II. Bachelor's thesis details

Bachelor's thesis title in English:

Application potential of NIR to IR optical centers in diamond

Bachelor's thesis title in Czech:

Aplikační potenciál NIR to IR optických center v diamantu

Guidelines:

1. Get acquainted with the current state of the near-infrared to infrared emitting optical (color) centers in diamond – fabrication and fundamental physical properties.
2. Using literature, compare the methods and elements for fabrication of active NIR-IR optical centers in diamond.
3. Using the literature, examine and analyze strategies for elements (such as Ni, Ni-Si, Ti, Xe) incorporation into diamond during the diamond growth process.
4. Fabricate a set of thin diamond films and examine their morphological and chemical character using SEM, Raman, and photoluminescence measurements.
5. Based on the literature review, summarize the challenges and outlooks of near-infrared to infrared optical centers in diamond for applications (e.g., Biology, medicine).

Bibliography / sources:

[1] A.M. Zaitsev, Optical Properties of Diamond: A Data Handbook. Springer, 2001
[2] S. Tóth et al., Journal of Luminescence, 2016, 176, 367
[3] T. Gaebel et al., New Journal of Physics, 2004, 6, 98; PII S1367-2630(04)77078-0.
[4] S. Pezzagna et al., New Journal of Physics, 2011, 13, 035024
[5] R. Sandstrom et al., Optics Communications, 2018, 411, 182.
[6] I. Aharonovich et al., Advanced Optical Materials, 2014, 2, 911.
[7] T. Iwasaki et al., Physical Review Letters, 2017, 119, 253601.
[8] S. Ditalia Tchernij et al., ACS Photonics, 2018, 5, 4864.
[9] M.E. Trusheim et al., Physical Review B, 2019, 99, 075430.

© ČVUT v Praze, Design: ČVUT v Praze, VIC

CZECH TECHNICAL UNIVERSITY IN PRAGUE

FACULTY OF ELECTRICAL ENGINEERING CTU IN PRAGUE

Faculty of Electrical Engineering
Program: Electrical Engineering and Computer Science

Study Year: 2020/2021 Study

Project of: Ramil Farzaliyev
Supervisor: Ing. Štěpán Potocký, Ph.D.

Bachelor Thesis

Application potential of NIR to IR optical centers in diamond

Declaration: “I hereby declare that this master’s thesis is the product of my own independent work and that I have clearly stated all information sources used in the thesis according to Methodological Instruction No.

1/2009 – “On maintaining ethical principles when working on a university final project, CTU in Prague“.

Date: Signature:

Prague, 2025

Contents

LIST OF ABBREVIATIONS

PL – photoluminescence

NV –nitrogen-vacancy

Si-V – silicon-vacancy

Ni – nickel

NE8 - nickel-related center surrounded by four nitrogen atoms

Ni-Si - nickel–silicon-related color center

ZPL – zero phonon line

CVD – chemical vapor deposition

HPHT – high pressure high temperature

HFCVD – hot filament chemical vapor deposition

MWCVD – microwave plasma chemical vapor deposition

FWHM – full width at half maximum

PECVD - plasma enhanced chemical vapor deposition

TS – substrate temperature

SIMOX – separation by implantation of oxygen

ABSTRACT

Owing to its outstanding physical and chemical properties, diamond has been of great interest for various technological applications, such as quantum computing, secure communication, sensing, and bio-imaging. This dissertation investigates the synthesis and characterization of diamond films, particularly those with such optically active defect centers emitting in NIR- to IR-region. Special focus is given to the silicon-vacancy (Si-V) and nickel-related (Ni) color centers, which are known to have excellent optical characteristics with remarkable photostability, narrow linewidth emission, and room-temperature quantum capability.

Experimental synthesis of diamond films has been synthesized by MWCVD and optimized with respect to the substrate temperature, deposition time, process gas composition, and silicon doping level. The surface morphology and crystallinity were investigated by scanning electron microscopy (SEM), and surface roughness was measured by AFM (atomic force microscopy), Raman and photoluminescence (PL) spectroscopy was used for the analysis of the structural quality and the optical properties in the synthesized films.

It is found that dense and high-quality Si-V centers have successfully been shaped, which indicates that they can be integrated into quantum photonic circuits, single-photon sources, and advanced biomedical imaging devices. This study enhances the understanding of the mechanisms involved in the formation of the color centers and sets the principles to optimize the processes of synthesis that are key for future technological applications.

INTRODUCTION

The development of modern society is closely intertwined with the development of information technology. Computers have become an integral part of our reality. Recently, a big leap has occurred in the field of mobile cellular networks and mobile data. With the increasing availability of information, the issue of its security is becoming more acute. One possible solution to the problem is the development of quantum communication lines [1] that allow the protection of transmitted information at the level of fundamental physical laws. The principle of protection of quantum communication lines is based on the impossibility of copying a single quantum state [2], which protects information from copying by intruders. Quantum communication lines at a distance of up to 150 kilometers have been implemented [3]. However, due to the exponentially increasing losses in the fiber transmission channel with the length,

to create a network capable of operating over long distances, quantum repeaters are needed that allow copying quantum information, but at the same time, provide protection against eavesdropping by intruders. Various types of repeaters reduce the exponential dependence of the loss on the distance to a polynomial one. The implementation of such systems requires reliable quantum memory and sources of determinism, including single-photon and mixed states of light. Despite the existence of experimental demonstrations of individual elements, their use is limited by the lack of technology for effective and reliable interfaces for interacting with the quantum systems underlying them.

The development of computing systems has a natural development in the field of quantum computing. The idea of quantum computing was first proposed in 1976 by Roman Ingarden [4]. A little later, in his 1981 lecture at the Massachusetts Institute of Technology, R. Feynman notes [5] that it is impossible to effectively model the evolution of a quantum system on a classical computer and suggested using a quantum computer for this task. Currently, the method of increasing the speed of calculations by reducing the size of the transistor is experiencing increasing difficulties in maintaining the performance growth of computing systems in accordance with Moore's law [6]. One of the promising solutions to the problem is the idea of using instead of the discrete logic of bits 0 and 1, quantum logic that operates with all possible superpositions of 0 and 1 in the complex space. It is shown that such machines are able to effectively solve problems that are difficult to solve for a classical computer, for example, the problem of decomposing a large number into prime factors [7] or calculating energy levels of complex molecules which opens up new opportunities for improving the speed and accuracy of calculations. The efficiency of quantum simulators and quantum computing systems based on various physical systems has been experimentally demonstrated: cooled ions in the Pauli trap [8, 9], quantum dots, color centers in diamond [10], and other systems. However, the creation of a mass computer of a new generation will require the use of solid-state chip compatible technology.

Among the many candidates for a quantum memory cell, diamond color centers have several competitive advantages that make them one of the most promising candidates for use in quantum applications.

The French naturalist of the XVIII century Lavoisier wittily showed what a diamond is made of. He focused the sunbeam on a crystal in a sealed flask, and when it burned, only carbon dioxide remained in the container. It turns out that the diamond is made of carbon. It seemed that everything was simple: you need to figure out how to turn soot, which was a lot in those days, or graphite into a crystal. But that was not the case. Diamond is the hardest mineral in nature, and graphite is one of the softest. Both are made of carbon. How to turn graphite into a diamond? The physicists measured the heat capacity of both minerals, performed thermodynamic calculations, and obtained the equation of the transition curve. By the 1930s, it became clear that the synthesis of diamond required very high pressures and temperatures, unattainable at that level of technology.

The real breakthrough came in the post-war years. The problem was solved in three technically developed countries that did not have their own diamond deposits in those years: Sweden, the United States, and the USSR. They had to be purchased abroad. The Soviet state set the task of diamond synthesis in 1947. But things were moving with a creak until in 1955, the article "Man-made diamond" appeared in Nature [11]. The authors are scientists from General Electric, including Tracy Hall. The company produced incandescent lamps, and diamond spinners were used to draw tungsten filaments. After this publication, the Swedish company ASEA said that it had synthesized diamond back in 1953.

It is very difficult and expensive to grow large jewelry diamonds, so they are unlikely to replace natural ones in the foreseeable future. High-tech applications are another matter.

Diamond has very suitable properties for solid-state microelectronics. Diamond is a wide-band semiconductor, resistant to high temperatures and radiation, with a thermal conductivity five times greater than copper. Moreover, there exist hundreds of color centers in diamond with specific properties. Relevance of the study. Impurity color centers in diamond have unique spectral characteristics: high brightness and stability at room temperature, high quantum efficiency, short photoluminescence (PL) attenuation times and narrow lines, and are of interest for nanophotonic and quantum optics.

Impurity color centers in diamond have unique spectral characteristics: high brightness and stability at room temperature, high quantum efficiency, short photoluminescence (PL) attenuation times, and narrow lines, and are of interest for nanophotonic and quantum optics [12]. The most intensely investigated centers are nitrogen-vacancy (NV) and silicon-vacancy (SiV) centers [13]. Also, Ni-based centers are a potential source of single coherent optical photons for quantum networks and are actively being developed as stable luminescent bioimaging probes based on their room temperature luminescence brightness and stability.

To realize these applications, controllable synthesis of material with bright and narrow PL lines is demanded.

However, similar to other transition metal-related centres, such as Ni, the fabrication of large-area diamond films containing Ni centres with uniform and controlled distributions is still a challenge.

The search for new sources of photoluminescence in the diamond matrix is still ongoing to expand the spectral range, increase the lifetime and efficiency of the PL to create high-power X-ray imagers (scintillators) in a transparent and heat-conducting diamond matrix, as well as bright biomarkers with a chemically and biologically inert diamond shell. However, the existing methods of doping diamond with rare-earth elements do not allow us to obtain a high signal-to-noise ratio PL [16].

Purpose of the work: the study of the synthesis processes of diamond films in microwave plasma with a gaseous precursor and study the structure, phase composition, and optical properties of the obtained materials.

Chapter 1. Literature review

Structure and properties of diamond

Information given in this subsection are based on references [17]

Diamond is the hardest substance in the world. It is a crystalline form of carbon with a unique combination of physical and chemical properties. Diamond is transparent to a wide range of radiation (from ultraviolet to far-infrared), is ch,emically inert and has an extremely high thermal conductivity – and these are just the most well-known of its properties, thanks to which it is used in many fields of science and diamondology. Diamond crystal lattice is cubic face centered. Each node of the lattice is

associated with a primitive basis consisting of two carbon atoms with coordinates 000 and $\frac{1}{4}\frac{1}{4}\frac{1}{4}$ all atoms are in the state of sp^3 – hybridization.

The space group of the diamond symmetry $F\ d3m$. The crystal facets are dominated by (111), (100), and (110) facets, forming an octahedral, cubic, and rhomb dodecahedral crystal appearance, respectively. There are also facets (211), (311), (221), (322), (332), (511).

Main characteristics of the diamond

- Chemical inertia (insoluble in hydrofluoric, hydrochloric, sulfuric, and nitric acids), but the contact of diamond with iron, nickel, cobalt, and platinum group metals at temperatures above 800 oC leads to the gradual dissolution of carbon atoms in the metal
- Radiation resistance
- Hardness (highest among known substances): 90-100GPa (single crystal)
- Thermal conductivity: up to 2400 W/m*K for a single crystal (at room temperature higher than that of any other bulk material)
- Young's modulus: 1200 GPa
- Debye temperature: 2000 K
- Melting point at vacumn: 3700-4000 °C at a pressure of 11 hPa
- Combustion temperature in the air: 850-1000 °C
- Coefficient of linear thermal expansion: 1.5-4.8*10^{-6} 1/°C (single crystal)
- Refractive index: 2.41
- Dispersion: 0.044
- Optical transparency in the range of 225 nm < λ < 2.5 microns (single crystal, the highest among known substances), optical isotropy
- Air friction coefficient: 0.05–0.15
- Band Gap: 5.45 eV (dielectric)
- Density: 3.515 g/cm^3 (single crystal)
- Electron mobility: 2200 cm^2/(V*s)
- Permittivity: 5.7
- Hole mobility: 1600 cm^2/(V*s)
- Biological inertias
- Superconductivity under boron doping (Tc ~ 4 K)

Carbon is a group IV element of the periodic table, contains 6 electrons located at two energy levels, the electronic configuration of the orbitals is $1s^2 2s^2 2p^2$. In the unexcited state at the lower level, there are 2 electrons with opposite spins on the spherical s-orbital, at the upper level there are 2 electrons on the sorbital and 2 unpaired electrons on three mutually perpendicular dumbbell-shaped p-orbitals. The atomic orbital is the part of space in which the probability of finding an electron is maximum.

Usually, a carbon atom is in an excited state: one electron from the upper s-orbital passes to the free porbital, thus the number of unpaired (valence) electrons increases to 4.

There are 3 different geometries of carbon electron orbitals, depending on the degree of hybridization:

- Sp^3-hybridization (tetrahedral, diamond structure, angle between orbitals 109° 28’). Four hybrid orbitals of equal shape and energy arise when one upper s - and three p - orbitals are mixed. This

hybridization in the solid leads to the formation of four strong σ-bonds. Configuration of carbon atom orbitals in diamond 1s24(sp)3 is in Figure 1.1.

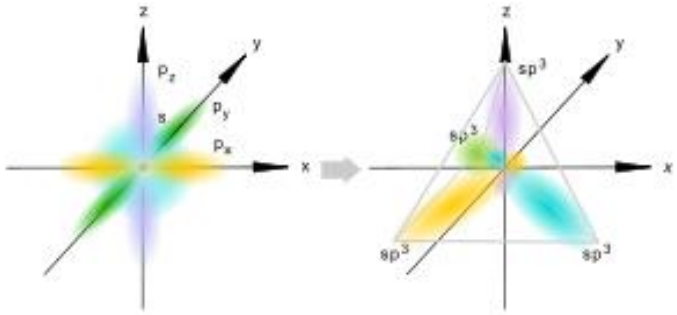

Figure 1.1 sp3-hybridization

- Sp^2-hybridization (trigonal, structure of graphite, graphene, fullerenes, nanotubes, nanofibers, angle between orbitals 120o). Three hybrid orbitals of the same shape and energy located in the same plane arise when the upper s - and two p - orbitals are mixed. In a solid, three hybrid orbitals are involved in the creation of three σ-bonds. The fourth p-orbital, which is not involved in iridization, is in the perpendicular plane and is involved in the creation of a weak p-bond (Figure 1.2).

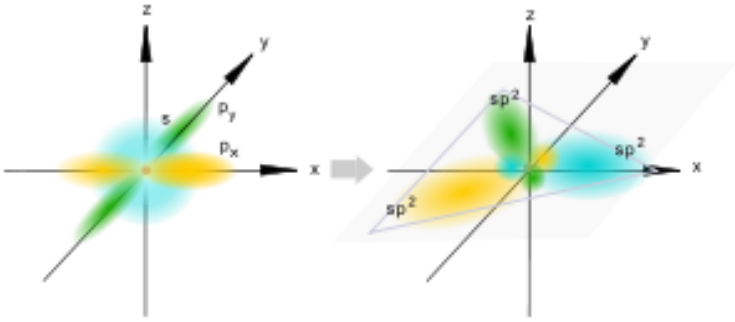

Figure 1.2 sp2-hybridization

- Sp-hybridization (diagonal, carbine structure). Two hybrid orbitals of the same shape and energy located on the same straight line arise when the upper s - and one p - orbitals are mixed. In a solid, two hybrid orbitals are involved in the creation of σ-bonds. The two-remaining p-orbitals create pbonds (Figure 1.3).

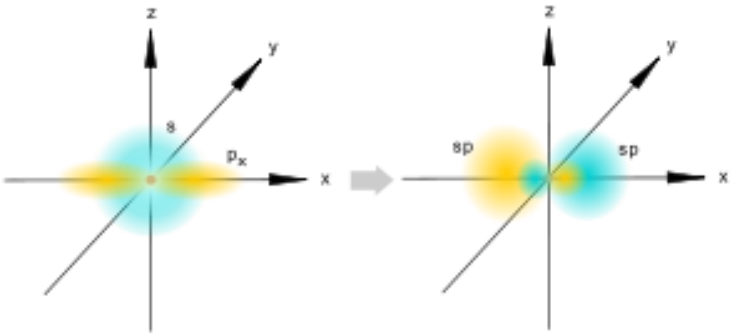

Figure 1.3 sp-hybridization

Carbon can exist in various allotropic modifications [18]:

1. Crystalline carbon
    a. Diamond (cubic crystal system)
    b. Graphite (hexagonal crystal system)
    c. Carbine (a linear chain based on sp-hybridization)
    d. Lonsdailite (a hexagonal polymorphic modification of diamond)
    e. Nanocarbon clusters (fullerenes, fullerite, nanotubes, nanofibers, nanodiamonds, etc.)
2. Amorphous carbon (αC) - coal, soot, coke, glass carbon, carbon nanofoam, etc.
3. Cluster forms (astralenes, diocarbon, carbon nanocones, etc.)

Almost all the physical properties of a diamond depend on its crystal structure. Each parameter has a maximum value in a single crystal, and when switching to a polycrystal, this value decreases. For example, the mobility of holes at room temperature decreases from 1600 cm2/(V*s) (for monocrystalline) up to 70 cm2/(V·s) (for polycrystalline) CVD diamonds. Moreover, the more ordered the grains of a polycrystalline film are, the higher the transport properties of such films will be. Of course, the mobility of charge carriers is also strongly influenced by ionizing impurities, which act as scattering centers (the mobility of carriers is approximately inversely proportional to the concentration of the impurity). Also, the electrical and mechanical properties of diamonds correlate with the density of structural defects.

Diamond application areas

The main areas of application of diamond are still jewelry and the production of abrasive tools. In cutting tools, such characteristics of diamond as the highest hardness and modulus of elasticity, low

compressibility, high wear resistance and low coefficient of friction are particularly appreciated. With many materials, metal Matrix Composite (MMC), aluminum-silicon alloys and tungsten carbide on a cobalt bond (WC-Co) [19]. Tungsten carbide is considered the most suitable substrate for creating diamond cutting tools [20]. The main disadvantage of WC-Co is the strong solubility (0.2-0.3 %) of carbon in cobalt and, as a result, poor adhesion of diamond to the substrate [21]. In addition, the presence of metallic cobalt suppresses the nucleation of diamond, catalyzing the formation of graphite. These effects can be partially offset by etching Co from the substrate surface in the Murakami reagent [22].

The electrical properties of diamond – the high drift velocity of charge carriers and the electric breakdown field strength, the large band gap (5.4 eV) make it a serious competitor to traditional materials used in electronics [23]. Due to its high radiation resistance, diamond is a suitable material for use in the space and nuclear industries (thermistors, detectors and dosimeters of ionizing radiation, etc.).

Diamond is also used in laboratories as a deterrent in high-pressure experiments, in high-performance bearings, diamond windows provide protection in experiments using acids or molten plastic [13]. The transparency of diamond windows in a wide range allows the use of measurement methods with infrared radiation.

After the synthesis of boron-doped semiconductor (p-type) diamond, transistors and diodes based on diamond were created. Currently, diamond electronics are primarily used in specialized applications, such as high-power, ultra-high-frequency (microwave) devices capable of operating under extreme conditions

— including exposure to radiation, high temperatures, and pressures — as well as in detectors of various types of ionizing radiation. [24].

In the work [25], the possibility of forming one - and two-dimensional optical resonators in thinned ion beam doped diamond films separated from the substrate (diamond membranes) by a system of nanoholes with a diameter of 150 nm is demonstrated.

More and more attention is being paid to promising biomedical applications of diamond. In fluorescence microscopy, organic dyes and fluorescent proteins are commonly used to visualize the functioning of biological systems at the molecular level [26]. But the duration of in-vitro and in-vivo observation is very limited, since organic and biological compounds are rapidly exposed to photobleaching. Semiconductor quantum dots are also promising drugs that have high photobleaching thresholds. Unfortunately, most quantum dots are toxic and insoluble in water [27]. To increase water solubility and reduce toxicity, surface modification is necessary, which inevitably changes the photophysical properties of the material.

Nanodiamonds have high biocompatibility with low cytotoxicity [28]. In addition, the diamond surface can be easily derivatized by a wide range of functional groups. Surface-functional nanodiamonds provide a versatile platform for conjugation with biomolecules such as peptides, proteins, and DNA. All this made it possible to create medicines and gene delivery systems based on diamond [29]. In addition to therapeutic applications, nanodiamonds can be used as markers of light scattering due to the high refractive index and the unique Raman signal of the diamond. Even more promising is the use of color centers in diamond as markers for optical bioimage [30]. In 2009, far-field fluorescence microscopy was used to successfully obtain images of the 3D distribution of NV centers in diamond with a distance of 120 nm from the resolved spots [31].

The biocompatibility of diamond along with its excellent electrical properties makes it the best material for electrical interaction with human neurons [32].

Among the more than one hundred color centers registered in diamond, the negatively charged silicon vacancy center (SiV-) is of particular interest, since its radiation is in a window for convenient bioimage. The center emits an intense narrow phonon-free line at a wavelength of 738 nm, well separated from cellular autofluorescence. Moreover, it is perfectly photostable, does not show any signs of photobleaching, even with powerful excitation of nanodiamond particles with sizes up to 1.6 nm [33].

The use of diamond-based optical interfaces as quantum detectors, storage, transmission and processing machines has recently exploded. Of all the color centers, nickel-related (Ni) centers in diamond have been studied widely because of their potentials for quantum technological devices.

Ni-based optical centers, such as NE8 and Ni–Si complex, have shown promising in quantum communication and quantum information processing, owing to their excellent optical properties. For example, these comprise bright single-photon emission, stable room-temperature photoluminescence, and emission predominantly localized to a narrow zero phonon line (ZPL) between 767 and 865 nm [14, 15]. The spectral narrowing and sharpening of protein-free Ni-related centers leads to high indistinguishability of the emitted photons, which is crucial for quantum cryptography and quantum networking applications [34].

With recent progresses single Ni centers can now be fabricated and integrated into photonic circuitry to deterministically control and optically couple these emitters to integrated photonic devices. Controlled

generation of the Ni-related optical centers were achieved by photolithography with chemical vapor deposition (CVD) and precise ion implantation followed by annealing. With such method, it has become possible to deterministically place and selectively address individual single spin centers associated with single Ni point defect centers in their diamond-photonics and quantum-computing devices [34].

Because of the high photostability and the weak electron-phonon interactions, the Ni-based color centers are promising candidates for coherent photon emission and quantum memory (quantum registers) of quantum optics applications. Their optical transitions are sensitive to the magnetic, electric and microwave fields allowing us to precisely control the quantum states. Recent experimental realizations have been carried out for quantum state initialization, coherent manipulation and read-out of single Ni-related emitters in room temperature settings, which reveals their most significant applicability to quantum nanotechnology [Neu et al.

And the Ni-related centers can provide new supports for ultrahigh-sensitive quantum-sensing, such as magneto-sensitivity and thermos-sensitivity, because of their magnetic property as well as temperature-dependent photoluminescence. Of particular interest are these high resolution, non-invasive experiments required for biological sensing and imaging purposes [34].

Further advances in diamond doping and photonic integration technologies suggest that Ni-based color centers may continue to push for quantum optical networks, quantum computing platforms, advanced sensing devices, in the future.

Zero phonon line

Information given in this subsection are based on references [35].

Phonon-free or Zero-phonon lines (ZPL) are narrow lines in the absorption and emission spectra of impurity luminescence centers (atoms, ions, or molecules in crystalline or disordered solid matrices) that occur during optical radiative quantum transitions between the energy levels of the center and occur without the participation of matrix phonons. In general, the spectral band corresponding to the electron (for molecular centers - electron-vibrational) transition in the impurity center consists of a narrow peak and a relatively wide spectral distribution-the phonon wing, due to transitions accompanied by the birth or destruction of the phonons of the matrix. The narrow ZPL in the spectra of the impurity centers are often called optical analogues of the resonant lines in γ-spectra observed in the Mossbauer effect. Currently, synthetic diamond is available in various shapes and sizes: single crystals, polycrystals with grains ranging from nanometers to hundreds of micrometers, as well as powders of various grain sizes. This diversity has stimulated research and attempts to apply diamond in a variety of fields, such as electronics, optics and lasers, quantum computers and cryptography, biology and medicine, high-pressure engineering, heat sinks, tribology, electrochemistry and corrosion protection, thermal field emission, electroacoustics, microelectromechanical devices, radiation, and chemical sensors.

Photoluminescence of diamond defects

Synthetic diamond containing optically active defects (color centers) is a promising material for use as a source of single photons in quantum information technologies [36], as well as luminescent markers in

biomedical technologies. So far, the main efforts of researchers have been focused on the study of negatively charged defects consisting of a substituting nitrogen atom and a vacancy in the neighboring node of the diamond lattice (the so-called $(N\text{-}V)^-$ centers), which give in the PL spectrum a pronounced ZPL at a wavelength of 637 nm and an intense phonon band shifted to the red region of the spectrum, associated with a strong electron interaction [37]. Other well-known color centers that allow obtaining intense PL in diamond are silicon-vacancy (SiV) defects with a ZPL at 738 nm and nickel defects with a ZPL at 802 nm. A special feature of these two types of defects is the weak electron phonon interaction [38].

Si-V defects (the Si atom and the vacancy are in neighboring lattice sites) are characterized by highly stable and narrow-band luminescence with a quantum yield of ~ 10% at room temperature, which makes them promising for use as luminescent biomarkers provided that the size of silicon-doped diamond nanoparticles is sufficiently small. The thermodynamic stability of Si-V defects is high not only for bulk diamond crystals, but also for diamond nanoparticles <10 nm. Silicon atoms, embedded in the diamond lattice, stimulate the formation of vacancies in neighboring nodes. Thus, Si-V centers are effectively formed directly when diamond is doped with silicon. Today, an urgent task is to find a controlled and effective method of alloying synthetic diamonds with silicon.

Defects associated with nickel (Ni), nickel–silicon (Ni–Si), titanium (Ti), and xenon (Xe) have also demonstrated photoluminescent emission in the near-infrared spectrum, in addition to silicon centers. Either ion implantation followed by thermal annealing or the introduction of nickel precursors during CVD growth are effective methods for forming Ni centers, such as NE8 and Ni_s^+, which emit at ~802–865 nm [14]. When both Ni and Si sources are present at the same time, co-doping with silicon produces Ni–Si complexes, which show sharp ZPLs at 767–775 nm and ~865 nm. These complexes can be efficiently produced during plasma-enhanced CVD growth of nanodiamond films [15].

HPHT diamonds have been found to contain Ti-related centers, such as Ti–N and Ti–V–N complexes, which are predicted to emit in the near-infrared spectrum. These are more challenging to synthesize consistently, though, and typically call for nitrogen co-doping and vacancy concentration control [39]. Since xenon is chemically inert, it usually enters through ion implantation and does not incorporate during growth. After annealing at high temperatures, Xe–V complexes are formed and show two distinctive ZPLs at 794 and 811 nm. Because nitrogen helps with charge compensation and stabilizes the defect complex, the emission intensity is noticeably higher in nitrogen-rich diamonds. [40]

By extending the available spectral range into the near-infrared, these centers enhance the extensively researched NV and SiV centers and are therefore highly relevant for quantum photonic and deep-tissue bioimaging applications.

Ion implantation

Information given in this subsection are based on references [41, 42]

Modern ion implants are an integral part of the equipment of most of the world's chipmakers, as well as advanced research laboratories that work in the field of micro and nanoelectronics. The implantation process is based on doping, or in other words, changing the electrical characteristics of silicon or other semiconductor wafers, which includes the formation of a beam of ions of the alloying element, its

acceleration and the introduction of these ions into the surface of the semiconductor wafer. As the path passes from the ion source to the surface of the plate, the ions can gain additional energy (accelerate) or, conversely, lose some of the energy. All this is due to alternating high- frequency or constant electric fields.

Ion implantation is usually performed at room temperature. As a result, a wide assortment of masks can be used for specific doping, such as silicon oxide, silicon nitride, aluminum, and photoresist

Ion implantation is used to create structures of the "silicon on insulator" type. In this case a process that has received the abbreviation SIMOX is used (Separation by Implantation of Oxygen) – separation by implanted oxygen. Large doses of oxygen atoms are implanted in a conventional silicon wafer. After annealing the plate, a layer of silicon oxide is formed, which serves as an insulator. Such structures are necessary in the production of electronic components. The implantation of silicon with cobalt, nickel, and iron ions is used to create magnetic nanoclusters and metal silicides. Composite materials based on magnetic nanoclusters are used in the development of new information storage elements. Metal silicides are also used as materials for contacts and interconnections of elements of integrated circuits.

The dose range is typically high at 10^{10} to medium at 10^{16} atoms / cm^2. The dose is an important parameter that characterizes the characteristics of the device and is very important for the beam current requirement. Generally, the higher beam current creates higher damage and changes sheet resistance after annealing. The phenomena are considered to come from two physical viewpoints. One is the change of diffuseness and the other is the change of activation owing to gathered damage. The change of sheet resistance cannot be effectively anticipated since it strongly depends on doped species, dose, and substrate temperature amid implants.

Diamond is a crystal characterized by extremely strong interatomic bonds. It is characterized by very small equilibrium parameters of the solubility of impurities and their diffusion coefficients. In this regard, ion implantation is a natural alternative to the doping method. Existing experimental data show that the p-type and p^+-type layer can be obtained by implanting boron ions. Implantation of Li+ and C+ ions leads to the formation of n-type layers. Diamond films grown in the presence of phosphorus and sodium can also have electronic conductivity. The efficiency of the introduction of electrically active centers differs significantly depending on the temperature of the diamond during implantation and on the mode of subsequent annealing [24].

Raman spectroscopy

Information given in this subsection are based on references [43]

Raman spectroscopy is a method of molecular spectroscopy based on the interaction of light with matter. It allows to get an idea of the material's structure or its characteristics. Raman spectroscopy is based on the study of scattered light. Raman spectroscopy provides information about intramolecular and intermolecular vibrations and helps to form a more complete picture of the reaction. Raman spectroscopy provides a spectral characterization of molecular vibrations ("molecular fingerprint") and is used to identify substances. At the same time, Raman spectroscopy can provide additional information about low-frequency modes and vibrations that indicate the features of the crystal lattice and molecular structure.

The principle of Raman spectroscopy

When light interacts with molecules in a gas, liquid, or solid, the vast majority of photons are scattered, having the same energy as the incident photons. This process is called elastic scattering. Some photons — about one in 10 million — after scattering acquire a frequency different from that of the incident photon. This process is called inelastic scattering or the Raman effect, named after Sir Chandrasekhar Venkat Raman, who discovered it and was awarded the Nobel Prize in Physics in 1930. Since then, the Raman effect has been widely used in various fields-from diagnostics in medicine to materials science and reaction analysis. The Raman effect allows you to learn the vibrational characteristic of a molecule, which gives you an idea of how it is arranged and how it interacts with other molecules.

The process of Raman scattering

From the point of view of quantum mechanics, the process of Raman scattering consists in the fact that when photons interact with a molecule, it can go into a virtual state with higher energy. There are several possible scenarios for the release of the molecule from this state. In one of them, a molecule can go to a state with a level of vibrational energy that is different from the initial level while emitting a photon with a different energy. The difference between the energy of the incident photon and the energy of the scattered photon is called the Raman shift.

If the energy of the scattered light decreases, such scattering is called Stokes scattering. Some molecules are initially in an excited vibrational state, and then after going to a virtual state with higher energy, they can go to a final state with an energy lower than that of the original excited state. Such scattering is called anti-stokes scattering.

High Pressure High Temperature diamond growth

Information given in this subsection are based on references [44]

In 1939, a thermodynamic calculation of the graphite-diamond equilibrium line was performed: The essence of the HPHT technology is as follows: graphite in a mixture with a metal (carbon solvent) is placed in a solid compressible medium. The required pressure (70,00080,000 atmospheres) is created by powerful hydraulic equipment. Heating is carried out to temperatures of

1500-2500 °C for two minutes. Diamond crystallization occurs due to the fact that the molten metal (iron) at high pressure and temperature turns out to be unsaturated carbon with respect to graphite and supersaturated with respect to diamond.

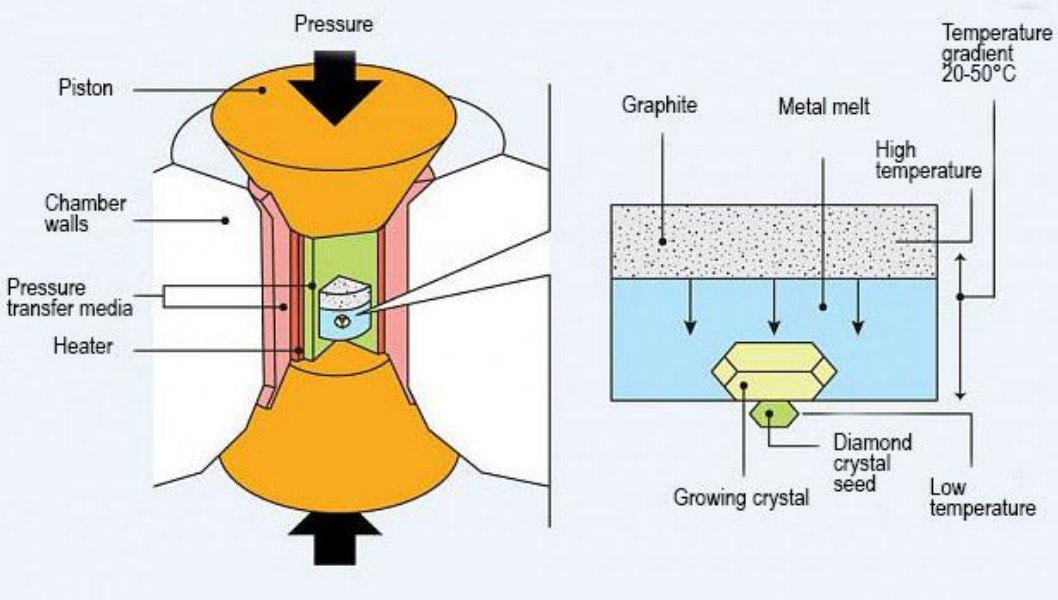

Figure 1.4 Diamond growing with HPHT

Under such conditions, it is thermodynamically more advantageous to form diamond and dissolve graphite. The raw materials currently obtained using this technology are mainly diamond powders with a grain size of 0.001-0.6 mm (maximum 2 mm) and a nitrogen concentration of more than 10^{19} cm^3. The first synthetic diamonds were produced in 1953 in high-pressure chambers. One of the variants of the modern design of such system is shown in Fig. 1.4. In the upper hottest part of the chamber, there is a carbon source – graphite, in the center there is a metal (Fe, Ni or Co), in the lower coldest part, there are seeds single crystals of diamond. An electric current through the heater is used to heat the melt to the desired temperature, and the hydraulic press creates the necessary pressure. When heated, the metal dissolves, and due to the difference in the solubility of carbon in the metal under the conditions of a temperature gradient, the carbon crystallizes on the seed crystals. The structure of such crystals is better than the best natural ones. However, the method still seems to have little prospects for obtaining diamond films and heterostructures. HPHT crystals remain the best substrates for epitaxy by CVD (Chemical Vapor Deposition), due to the perfection of their crystal structure. Another way to transfer carbon to the desired part of the phase diagram is the explosive decomposition of powerful mixtures of explosives under conditions of negative oxygen balance in a nonoxidizing environment. This is the cheapest way to get diamonds. In this way, nanodiamond particles are obtained, which are used for abrasives and sprays. In addition, detonation diamond is excellent for seeding the surface with nucleation centers before subsequent heteroepitaxy of polycrystalline diamond films in the CVD method. Among the advantages of the detonation method, it is worth highlighting the high performance, the absence of the need for expensive materials, such as catalyst metals or hard alloys. The obvious disadvantage is the danger of blasting, manufacturing and transportation of explosives.

There is a technique for the synthesis of microcrystals (6-9 microns) of a diamond from a suspension of hexagonal graphite in various organic liquid media under the influence of ultrasonic cavitation. Cavitation is the phenomenon of rupture of a droplet liquid under the action of tensile stresses when an intense ultrasonic wave is emitted into the liquid, i.e., the formation of gas-filled cavities. Depending on the cavitation conditions, at the moment of collapse of the cavitation cavities, the pressure p and temperature T inside the cavity can reach high instantaneous values, $p \sim 10^5 – 10^6$ bar, $T \sim 1000$ K [45].

Chemical vapor deposition

Since the mid-1950s, it has been possible to grow carbon materials using a wide range of chemical vapor deposition (CVD) techniques. This method allows the deposition of four different types of carbon: amorphous carbon (sp^2 hybridization, α-C), tetrahedral amorphous carbon (tα-C), polycrystalline and monocrystalline diamond films [46].

The main stages of the process of diamond deposition from the gas phase are shown in Fig. 1.5:

1. introduction of reagent gases into the vacuum chamber.
2. plasma, thermal or chemical activation (decomposition into active radicals).
3. transfer of active radicals and molecules to the growing surface; 4. chemical and diffusion processes on the surface; 5. deposition of diamond on the substrate.

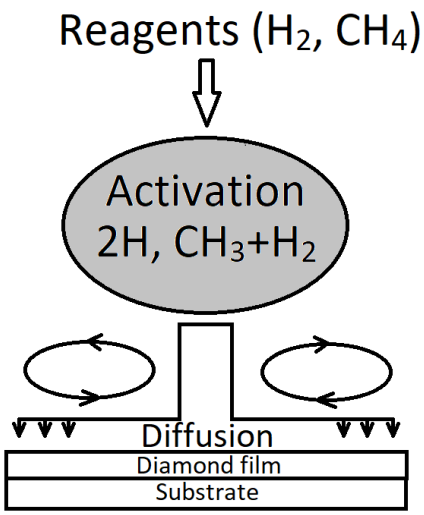

Figure 1.5 CVD scheme

In the CVD method, diamond deposition always occurs on the substrate. To obtain single-crystal films, single-crystal substrates are used. It is possible to grow diamond films with a thickness of hundreds of nanometers to several millimeters. Polycrystalline films are prepared by heteroepitaxy on non-diamond substrates, and the substrate is pre-coated with diamond seed particles – nucleation centers, for example, by ultrasonic treatment of the substrate in a suspension of nanodiamond powder obtained by detonation [47]. Heteroepitaxy of the diamond is also possible without the use of pre-seeding. In this case, the spontaneous nucleation of the diamond plays a decisive role [48]. The sizes of diamond crystallites in the grown films can range from 5 nm to hundreds of microns [49].

Hydrocarbons (usually methane, propane, acetylene, tetramethyl silane) are used as a carbon source. The process of diamond synthesis is weakly dependent on the type of hydrocarbon injected, and depends

mainly on the substrate temperature(700-1100 °C) [50], the ratio of reagent concentrations, and the pressure of the gas mixture (can range from fractions to hundreds of Torr), the geometry of the substrate holder and the gas activation power. Diamond deposition rate values by the CVD method, they range from fractions of a micron to hundreds of microns per hour.

The most important component of the deposition process of the diamond is hydrogen, which is supplied tens or even hundreds of times more than hydrocarbon. Methane or other hydrocarbon molecules are only needed to feed the carbon atoms [51]. The main function of hydrogen is to close the broken carbon bonds on the surface of the growing diamond. Hydrogen also activates the diamond surface by creating open carbon bonds ready for the addition of a hydrocarbon radical. In addition, hydrogen atoms can break down neutral hydrocarbons in the gas and create active radicals, such as CH_3 and CH_2, for example:

$CH_4 + H \leftrightarrow CH_3 + H_2$

The active hydrocarbon radical combines with an open carbon bond to form a trigonal sp2 (a-C, graphite) or tetrahedral (sp^3, ta-C) bonds [50]. Thus, in CVD synthesis, in addition to diamond, amorphous carbon and graphite are also formed on the growing surface. The high quality and purity of diamond films is achieved due to the fact that atomic hydrogen etches the graphite sp^2 phase of carbon much faster than the diamond-like sp^3 phase. Hydrogen also destroys long-chain hydrocarbon molecules, preventing the accumulation of polymers and large ring structures in the gas phase, which can be deposited on the growing surface.

To ensure a sufficient concentration of atomic hydrogen, the activation of the gas phase is required, for which mainly thermal or electrical methods are used. The substrate temperature in CVD diamond synthesis is limited on both sides by the approximate range of 800-1400 °C, since the deposition rate of diamond is insufficient at lower temperatures, and at higher temperatures the growth of graphite dominates. Depending on the activation method, the pressure and temperature of the gas, the substrate must be additionally cooled or heated. The disadvantages of the CVD method of diamond synthesis include inheritance of substrate defects by the epitaxial material, limited choice of substrate materials due to limitations in the synthesis temperature, the need to select a substrate with a CTP close to diamond for the synthesis of thin films, low deposition rate, explosive reaction gases.

The main advantages of the CVD method: the best purity and quality of diamond films in comparison with other methods, freedom from spatial growth restrictions, the possibility of controlled growth of the diamond phase on hetero-points, the possibility of precise doping of the grown films in a wide range of concentrations, the possibility of layer-by-layer doping without stopping the synthesis, the creation of heterostructures, the possibility of creating multicomponent composites, the possibility of applying one- and double-sided films on parts of complex shape and large area, the possibility of growth in stages with different synthesis parameters.

The method of producing diamond films by the CVD method is out of competition for most tasks of electronics, photonics, biology and medicine, the creation of heat sinks and surface treatment of special cutting tools.

To ensure a sufficient concentration of atomic hydrogen, the activation of the gas phase is required.

Methods of gas activation in the CVD process

Bachman et al. were the first to show that diamond synthesis is possible only in a small section of the C/H/O gas phase diagram [52]. Prijaya et al. [53] calculated the solubility of carbon in the gas phase by placing a graphite disk in hydrogen at constant pressure. In good agreement with the results. They showed that in the presence of temperature equilibrium and a uniform distribution of gas molecules, diamond growth and graphite removal depend solely on the ratio of carbon to hydrogen and oxygen concentrations in the reactor. However, in real CVD processes, the temperature distribution, solubility, and internal energy depend significantly on the type of activation. Thus, a significant difference in the CVD processes of diamond synthesis is based on different methods of gas activation or their combinations in hybrid systems that use more than one energy source. According to Spitsin et al. the activation of the gas phase can be based on heating (thermal and chemical activation) or plasma ionization (electrical and electromagnetic activation) (Figure 1.6) [54].

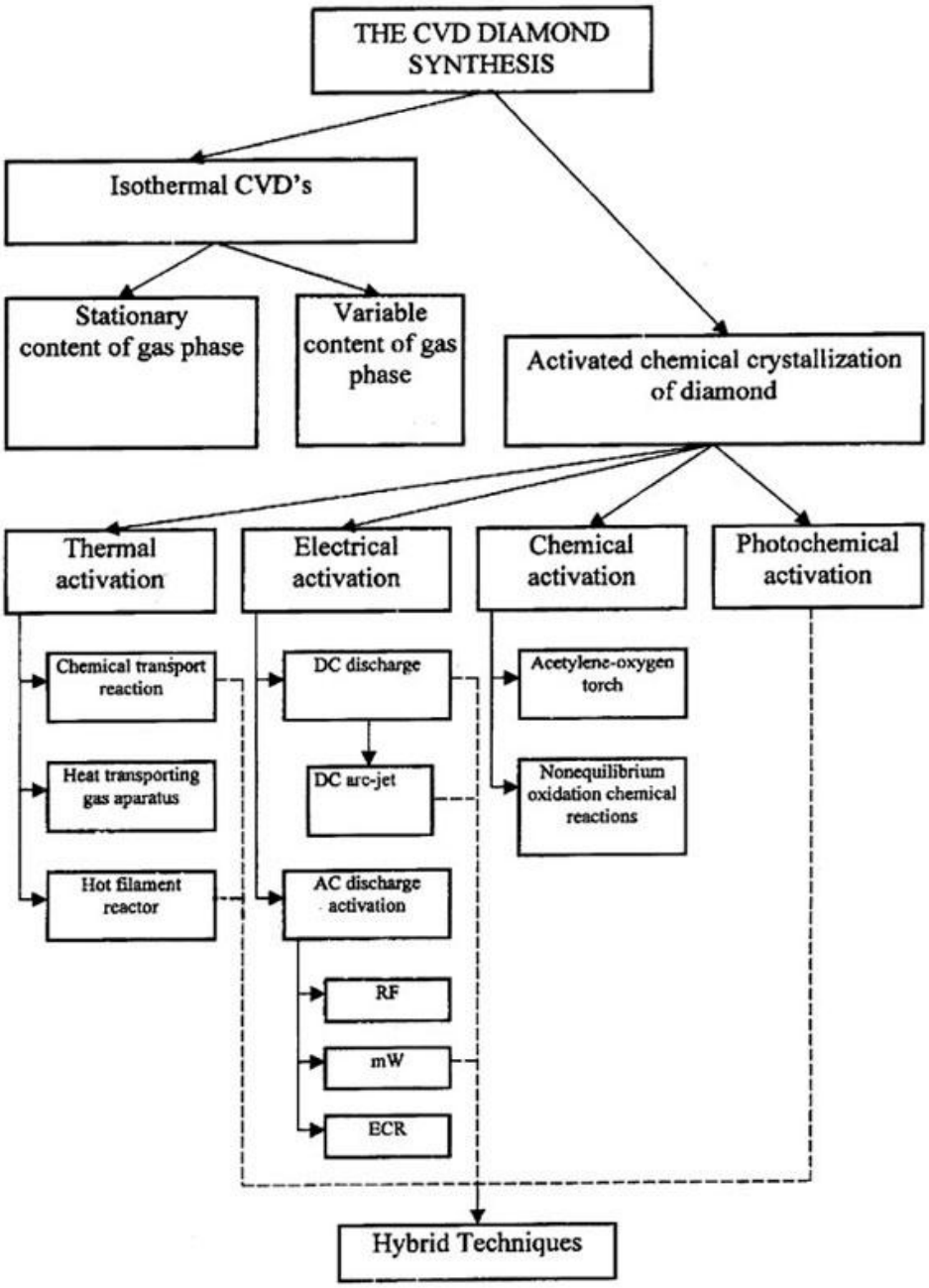

Figure 1.6 Methods of CVD synthesis of diamond [54].

In the process of thermal and chemical activation, the gas phase can be heated up to 3500 K. In the process of electrical and electromagnetic activation, the gas phase is ionized and forms a plasma ball or jet, stable molecules turn into neutral and charged particles: C_2H_2, C_2H_4, CH_3, C_2H, CH_2, C_2, CH+, CH_2 Hydrogen molecules dissociate into atoms and ions H^+, H_3^+ and H^-. The molecules and electrons in the plasma exist at different temperatures. Inelastic collisions between electrons and atoms create active radicals, while elastic collisions heat the gas. The plasma temperature can be estimated by spectrometric methods: the temperature values of electrons can reach 100,000 K, molecules-10,000 K [55].

During thermal activation, a wire made of refractory metals (W, Ta) heated to 2000-2200 °C is placed at a distance of 5-7 mm from the substrate heated to 700-1000 ° C [56]. This method is called the Hot Filament Chemical Vapor Deposition method (HFCVD) (Figure 1.7).

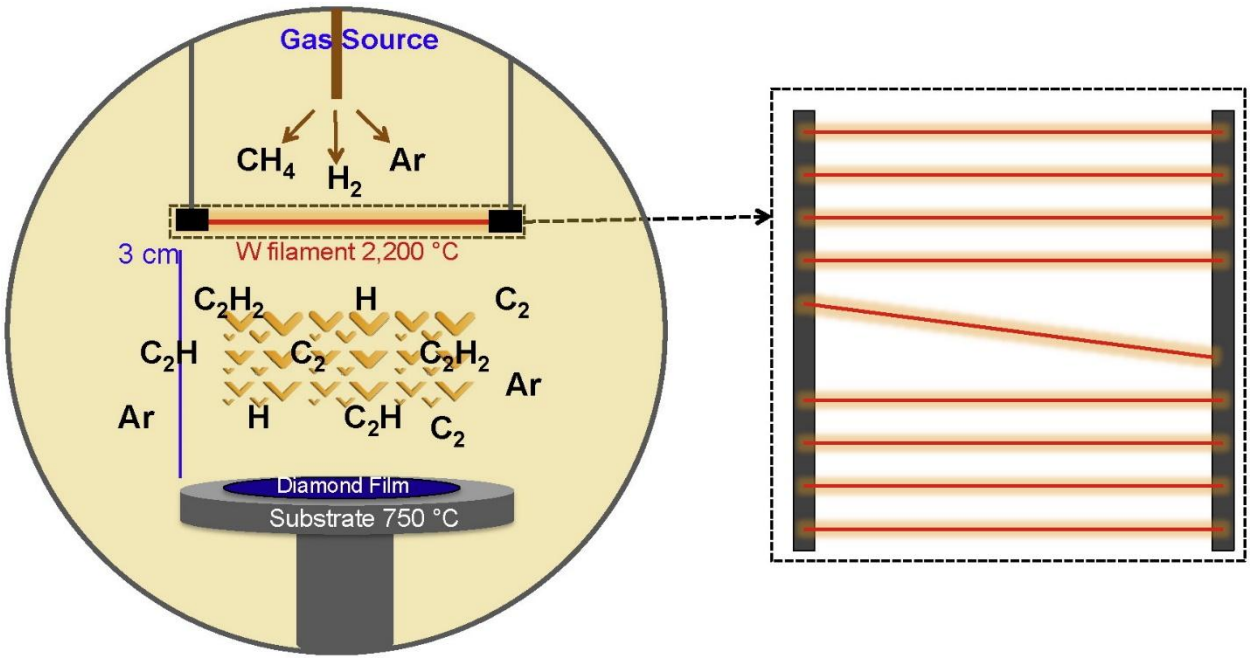

Figure 1.7 cross-section diagram of the HFCVD deposition chamber and top view of the filament array [57].

The pressure of the supplied hydrocarbon mixture is 20-60 Torr. The method is used for coating cutting, milling and grinding tools with micro-and nanocrystalline diamond films [58]. It is also possible to configure the installation when the carbon source is not a gas, but the heater itself: a graphite disk or a rod [59]. This process is called chemical transport (Chemical Transport Reaction, CTR) and has a serious drawback – it is impossible to control the concentration of carbon in the gas phase regardless of the activation temperature.

The reasons for the widespread use of HFCVD technology are the simplicity of the process, cheap equipment, good quality coatings and the ability to apply diamond films on a large area (more than 0.5 m^2 [57]). Among the disadvantages are the low growth rate (1 microns / hour), degradation of the thread, contamination of the gas mixture with the material of the heated thread and, as a result, contamination of the synthesized film.

During chemical activation in acetylene flame, the diamond is grown in the flame of an oxygen-acetylene burner on a substrate, which is installed on a water-cooled block (the method was first described in 1990, [60]). In the simplest case, the process is carried out at atmospheric pressure without using a reactor. The temperature of the burning flame reaches only values of 3550 K. As in the case of thermal activation, the internal energy is about 100 times lower than the ionization energy.

Advantages:

extremely high diamond deposition rates up to 100 microns / hour, no reactor required, easy setup, inexpensive equipment.

Disadvantages:

Small area (limited by the shape of the flame) of the deposited coatings, poor process control, strong heating of the samples. In order to increase the deposition area, techniques with multiple burners or with a flat flame at reduced pressure are used [61].

Despite the industrial advantages of this technique, most publications report only the success or failure of synthesis under certain experimental conditions. Several application-oriented works concern deposition on molybdenum and wolfram carbide [62] substrates to create a wear-resistant tool for processing aluminum alloys [63].

Another method utilizes **electrical activation** where two types of discharges in the gas are used: glow and arc. The main advantage of using a glow discharge is the low price of the equipment and the ease of its configuration. Disadvantages: small deposition area at high pressure, low growth rate at low pressure, contamination of diamond films with cathode material. The increase in pressure and power leads to a DC arc discharge between the cathode and the anode.

Glow discharge reactors consist of two electrodes that are located parallel to each other. The precursor gases, after being introduced into the reactor, are heated in the discharge between the electrodes, and the diamond is deposited on the substrate, which is part of the anode.

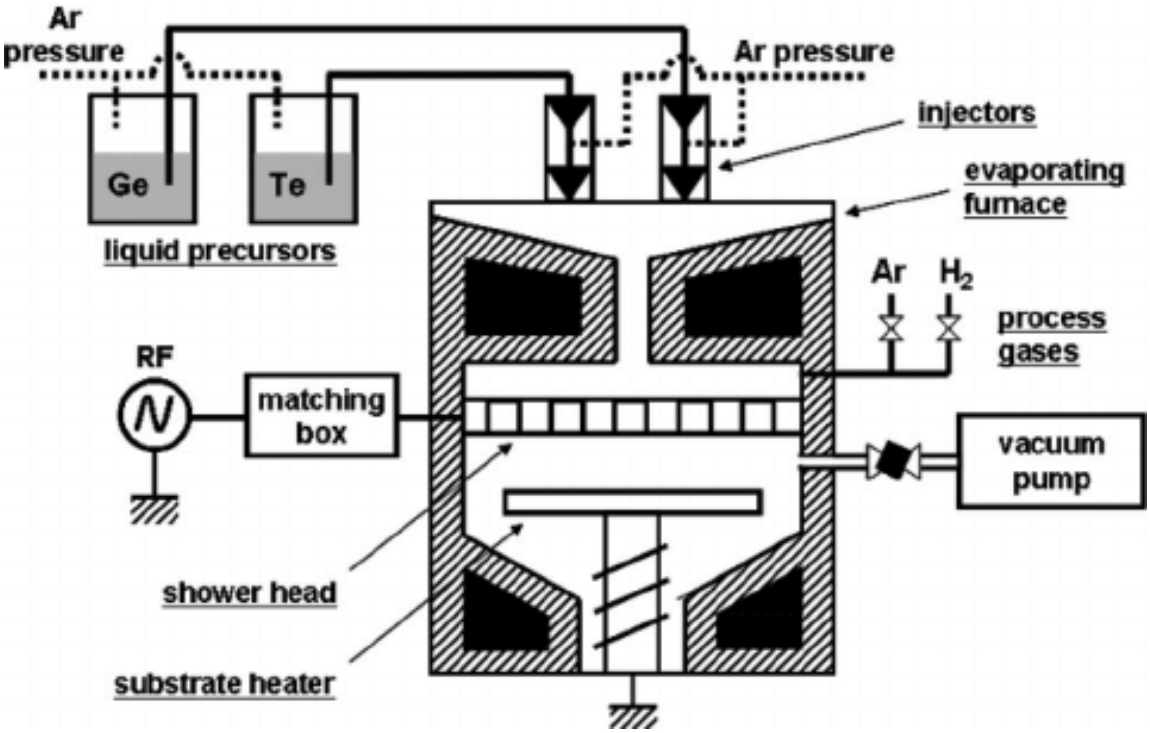

Figure 1.8 Structural drawing of the plasma CVD apparatus.

The main advantage of using a glow discharge is the low price of the equipment and the ease of its configuration. Disadvantages: small deposition area at high pressure, low growth rate at low pressure, contamination of diamond films with cathode material.

The increase in pressure and power leads to a DC arc discharge between the cathode and the anode. The installation diagram of the electric arc plasma torch is shown on Picture 1.8. Argon and hydrogen, heated in an electric arc discharge, flow out through the nozzle, forming a high-speed plasma jet with a temperature in the core of the flow up to 40,000 ° C, which is much higher than in gas activation methods using microwave plasma or hot filament. The carbon source (methane) is not simply injected into the reactor but is mixed directly with the plasma jet. Due to the high degree of decomposition of gases, diamond deposition rates reach record values (more than 900 microns / hour) [64]. Due to the limitations in the expansion of the plasma jet, it is impossible to obtain homogeneous coatings of a large area. The main source of impurities in the gas in electric arc methods is the "hot" spot of the cathode. Also among the disadvantages of this method is the difficulty of controlling the process, expensive equipment, high gas consumption and degradation of the electrodes.

An electromagnetic activation uses electromagnetic waves in a wide frequency range to excite gases. Among the publications, three main directions prevail:

- RF plasma from 3 kHz to 3 GHz (Radio-Frequency plasma enhanced Chemical Vapor Deposition, RFCVD) [65]
- Microwave plasma from 300 MHz to 300 GHz (Microwave Plasma Chemical Vapor Deposition, MWCVD) [66]. However, the frequency of 2.45 GHz [67] is usually used, since it is often used in industrial microwave heaters and is therefore available with high power laser plasma (Laser-Induced Chemical Vapor Deposition, LIPCVD) [68]. Different types of lasers are used: excimer (3000 THz, UV), Nd: YAG (281 THz, 1064 nm) [69] and CO_2 laser (28.3 THz)[68].

Mechanisms of electromagnetic wave absorption

In the CVD processes, the gas is present in the gaseous and plasma phases, which absorb electromagnetic waves in different ways. There are no free charge carriers in the gas phase, so it is heated by:

- Dielectric heating (dipole rotation) due to the ability of the electric field to polarize the dielectric and the inability of this polarization to follow extremely rapid changes in the electric field. In addition to the rotation, the dipoles of the molecules can absorb electromagnetic waves through vibrations. At a sufficiently high-power density, absorption can lead to an increase in the internal energy and ionization of the molecules in the gas [70].
- Multiphoton absorption - in this process, photoionization occurs as a result of the sequential absorption of several photons over a period of time determined by the uncertainty principle [71].

With the transformation of gas into plasma, the number of mechanisms of absorption and interaction increases:

- Reverse bremsstrahlung is the absorption of a photon by an electron in the vicinity of a charged particle, followed by the transfer of vibrational energy from the electron to the particle [72].
- Ohmic plasma heating – heating by an electric current passing through the plasma. Energy absorption occurs, as in reverse bremsstrahlung, as a result of collisions of accelerated electrons

with other particles inside the plasma. There are capacitance-coupled (Capacitance-Coupled Plasma, CCP) and inductive coupling (Inductive Coupling Plasma, ICP) reactors. In the first case, current fluctuations in the plasma occur between the plates of the capacitor [65]. An ICP reactor consists of a device that corresponds to a transformer, where the second coil has been replaced by a conducting plasma.

- Stochastic or collision less heating of the plasma – due to electrons reflected from the oscillating electron less region of the plasma of positive space charge.

CVD reactors with electromagnetic activation can be with point excitation of a high-speed gas stream flowing out of the nozzle and forming a plasma jet, or with the excitation of a plasma ball. To obtain a plasma jet, it is possible to use a radio frequency, microwave and laser plasma [73]. There are quite a lot of variants of reactor designs with the formation of a plasma ball and their development continues at the present time. The plasma ball is produced by the formation of a standing wave under resonance conditions inside the reactor and is located above the diamond deposition substrate. The vacuum chamber, the simultaneous absence of electrodes and other surfaces interacting with the plasma, make this activation method the «cleanest» in terms of the quality of the synthesized material. The plasma ball allows you to obtain homogeneous coatings of a large area. There are no fundamental restrictions on the area of the synthesized films, only a large reactor and a powerful microwave source are needed. The absence of degrading components allows you to maintain stable parameters of the synthesis process for hundreds of hours. All this makes the MWCVD method the best for the tasks of controlled diamond alloying and obtaining materials with specified luminescent properties.

Full Width at Half Maximum

Information given in this subsection are based on references [74].

The full width at half maximum (FWHM) is the width of a line shape at half of its maximum amplitude, as shown below:

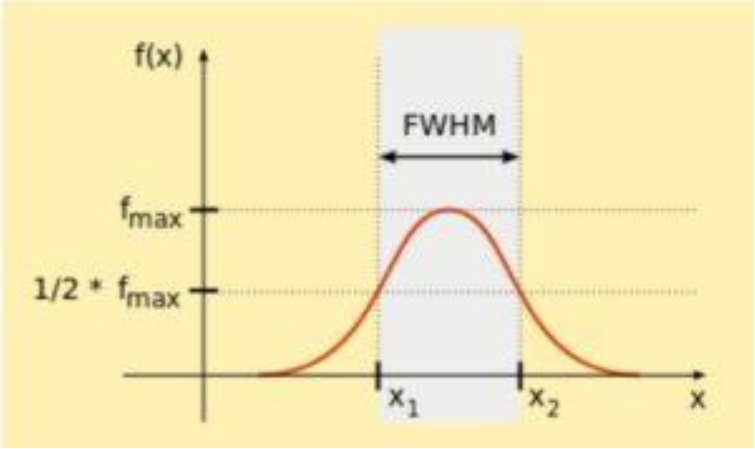

Figure 1.9 Full width at half maximum region of the peak.

A closely related quantity is the half-width at half-maximum (HWHM) or resolving power and is half the FWHM. For Gaussian line shapes, the FWHM is about 2.4 standard deviations. Although the concept is

simple, it is an important quantity; the FWHM is used to define resolution. If two peaks have overlapping FWHMs, they are not resolvable, i.e., they look like a single peak.

Ratio of FWHM to N-V centers have FWHM > 100 nm, while Si-V centers have FWHM < 10 nm.

Optically active defects in diamond

The introduction of defects and impurities into the diamond lattice leads to the formation of new energy transitions that affect the absorption and luminescence spectra of the material. A special type of impurity defect in diamond, which has recently received much scientific attention, is the family of "Impurity Vacancy" centers. The presence of such centers in diamond is usually accompanied by the appearance of intense narrow-band peaks in the luminescence spectra of the material [75]. The proportion of vacancy defects can be increased by irradiating the crystal with electrons, neutrons, or femtosecond laser radiation (leading to the mass formation of vacancies in the material), followed by high-temperature annealing in vacuum up to 1600 ^{0}C (stimulates the migration of vacancies inside the crystal).

The "impurity-vacancy" color centers in diamond are currently the subject of active research, taking into account the prospects for their application in quantum information technologies [76], optical biomarkers [77]. The most studied optically active defects for these purposes are impurity color centers, such as the nitrogen vacancy (NV), silicon-vacancy (Si-V) [12] and Cr which also allow obtaining intense photoluminescence in diamond. In contrast to the NV center, the negatively charged silicon-vacancy (SiV^-) center shows a weak electron phonon interaction, and 70% of its photoluminescence (PL) emission is at a few nanometers narrow PL zero-phonon line (ZPL) λ = 738 nm (half-width ~5 nm at room temperature) [12]. Also narrow-band photoluminescence (PL) of nickel (Ni)-related centers—surrounded by four nitrogen (N) atoms (NE8) and Ni–Si complexes—is observed in the range of the near-infrared (NIR) spectrum with low electron-phonon coupling. For instance, the center NE8 has a ZPL at 802 nm [78], while Ni–Si complexes have peaks at 767–775 and 865 nm in emission [14].

Initial work showed the creation of Ni-related centers by ion-implantation but with the added issue of introducing lattice damage and non-radiative recombination for optical properties [14]. More recently, the focus has transferred towards in situ doping during plasma-enhanced CVD, where nickel precursors are either inserted into the gas phase during growth. Under controlled plasma conditions, such silicon co-doped NiAg nanoparticles form reproducible Ni–Si complexes with high photostability and emission lines [15].

In addition, a number of other color centers associated with impurities, including those based on heavy metals, were found, and most of them are formed using ion implantation technology [79] which however has a serious drawback – residual radiation damage to the surface even after annealing. The structure of the disordered diamond around the doped atom can lead to poor reproducibility of the position of the impurity atom and a significant decrease in the intensity of its photoluminescence. In addition, the implantation method does not allow to obtain a uniform distribution of the impurity over the sample depth, to ensure deep penetration of the impurity (more than 10 microns) and to effectively introduce high concentrations of the impurity [13]. For the problems of diamond doping for electronics and optics, the CVD method is much better suited, however, it is quite difficult to embed a large atom in the densest diamond lattice among all crystals without significantly degrading its structure. The search for new color centers is of interest for expanding the spectral range and properties of already known luminescence

sources [80]. The center of the silicon-vacancy color (Si-V), in contrast to NV, is a point defect in the form of a silicon atom that has replaced two carbon atoms at once, and the silicon atom is in the interstitial position.

Silicon vacancy centers in diamond

So far, the main efforts of researchers have been focused on the study of defects consisting of a substituting nitrogen atom and a vacancy in the neighboring node of the diamond lattice (NV-centers), which give in the photoluminescence spectrum bright phonon less line λ=637 nm (negatively charged center NV^-), 575 nm (center without charge NV^0) and an intense phonon band shifted to the red region of the spectrum due to the strong electron-phonon interaction in the diamond lattice. Nitrogen has an anisotropy of the probability of inclusion in the diamond lattice during growth on the faces of crystallites with different crystallographic orientations [81]. The NV photoluminescence is distributed over a large side phonon band and only 4% of the total luminescence is in the zero-phonon line (ZPL). To fully utilize the capabilities of NV centers, they must be cooled to helium temperatures (4-10 K), which significantly limits the range of possible applications. Another feature of NV centers is the strong quenching of luminescence when the size of diamond particles decreases to values less than 25 nm. The center of the silicon-vacancy color (Si-V), in contrast to NV, is a point defect in the form of a silicon atom that has replaced two carbon atoms at once, and the silicon atom is in the interstitial position.

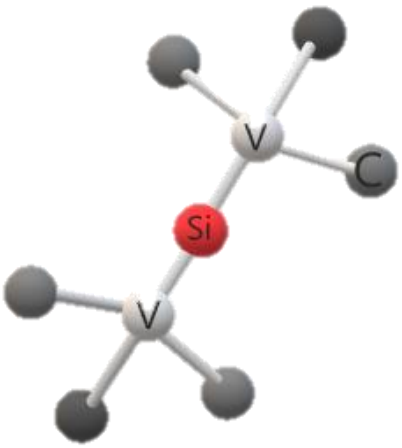

Figure 1.10 Silicon Vacancy centers in diamond

Silicon-like carbon, an element of group IV of the periodic table Mendeleev, has a carbon-like electronic configuration of the 3s outer orbitals $3s^2 3p^2$, a lattice constant of 5.43 Å and is the most intensively used material in modern electronics. Si-V defects are oriented in the diamond mainly along the direction <111> and since Si-V is a dipole, it exhibits a strong radiation direction, the maximum of which is observed orthogonally to the axis of the dipole <111>. For this reason, the efficiency of collecting the signal from the Si-V centers is higher from the diamond surface <111>.

The electron structure of the negatively charged center Si-V consists of one main $2E_g$ and one excited ^2E_u levels, each of which splits into a doublet thin structure at 0.194 and 1.068 MeV due to the spin-orbit

interaction (the interaction of the electron spin S = 1/2 and the orbital magnetic moment around the axis of symmetry (111) [82] (Figure 1.11).

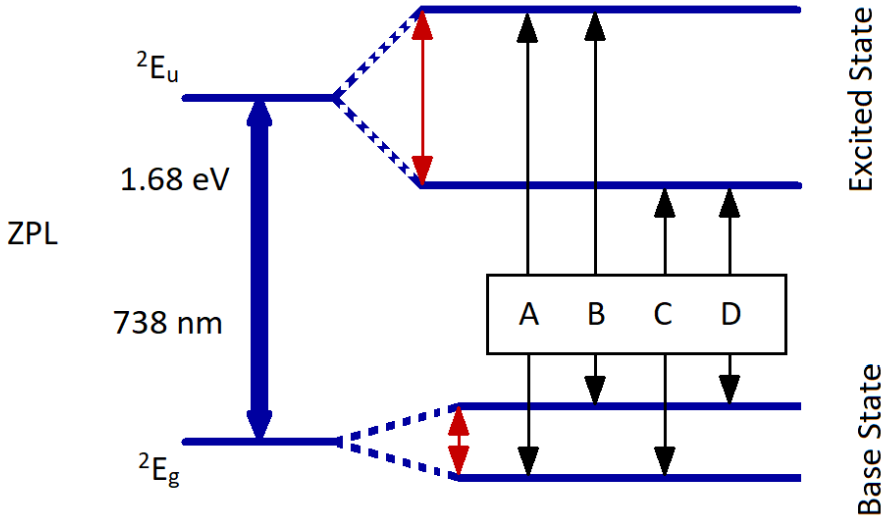

Figure 1.11 Diagram of Si-V- energy levels

Thus, the $^2E_g \leftrightarrow {}^2E_u$ transition results in a fine structure of four lines in the PL spectrum at wavelengths of≈736-737 nm (1.68 eV) with two different polarizations (Figure 1.12).

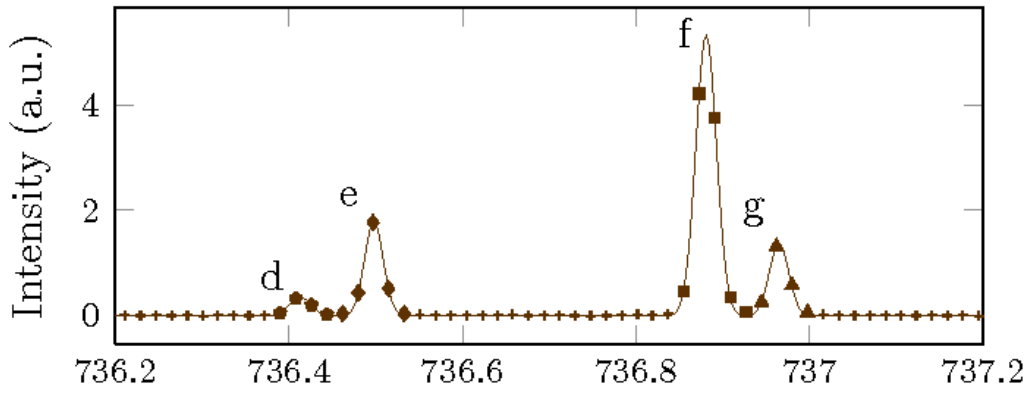

Figure 1.12 Fine structure of the Si-V- center [81]

In contrast to the NV center, the negatively charged silicon-vacancy center in diamond has a small phonon sideband, with 70% of its PL concentrated in a narrow phonon-free line at a wavelength of 738 nm (halfwidth ~5 nm at T_{room}). This is a significant advantage for applications requiring indistinguishable photons: quantum communications, photon-entanglement-based information processing, and qubit generation [83]. Si-V defects have high thermodynamic stability, not only for bulk diamond crystals, but also for diamond nanoparticles <10 nm [47]. Using the example of a meteorite diamond, it was shown that the luminescence of the Si-V centers is preserved even when the diamond particle size is less than 2 nm. Moreover, the radiation/absorption wavelength of Si-V centers is located in the transparency window

of biological tissues (650-1100 nm). Thus, diamond nanoparticles containing Si-V centers are an excellent material for creating luminescent biomarkers. In addition, Si-doped diamond films have excellent tribological properties due to a lower coefficient of friction compared to unalloyed or boron-doped films [84].

In contrast to doping with other elements, such as nitrogen (N), phosphorus (P) or boron (B), for which doping in the synthesis process is well studied, only a narrow range of works on controlled doping of diamond with silicon from gas in the CVD film deposition process can be found in the literature [85]. In these studies, it was found that films grown at sufficiently high silane concentrations have a more defective microstructure and contain a significant amount of the amorphous carbon phase. As an alternative to silane, tetraethoxysilane ($C_8H_{20}O_4Si$) was used for the deposition of diamond films on silicon substrates [85] and tungsten carbide substrates on a cobalt bond (WC-Co) [86] in hot-filament synthesis systems. The only indicator of successful Si doping in these films was the emission of photoluminescence of Si-V defects at a wavelength of 738 nm. Thus, the alloying of diamond coatings with silicon is an important direction for both photonic and mechanical applications.

Nickel vacancy centers in diamond

In the field of diamond photonics, a considerable concentration has historically been placed on NV and Si-V centers. However, another family of optically active centers, with enormous applications in quantum technologies and bioimaging, are the nickel-related (Ni-related) defects. Nickel can involve various color centers when doped into diamond, i.e., the Ni–silicon complex (Ni–Si), substitutional nickel (Nis +), and NE8 complex (Ni–N). Exhibiting distinct zero phonon lines (ZPLs) at around 770–870 nm, these defects generally emit in the near infrared (NIR) spectral window. This places them in the middle of the biological transparency window (650–1100 nm), ideal for deep tissue imaging. Ni-based centers like NE8 have weak phonon coupling and a relatively narrow ZPL, while NV has very strong phonon sidebands with only 4% of the total emission in the ZPL.

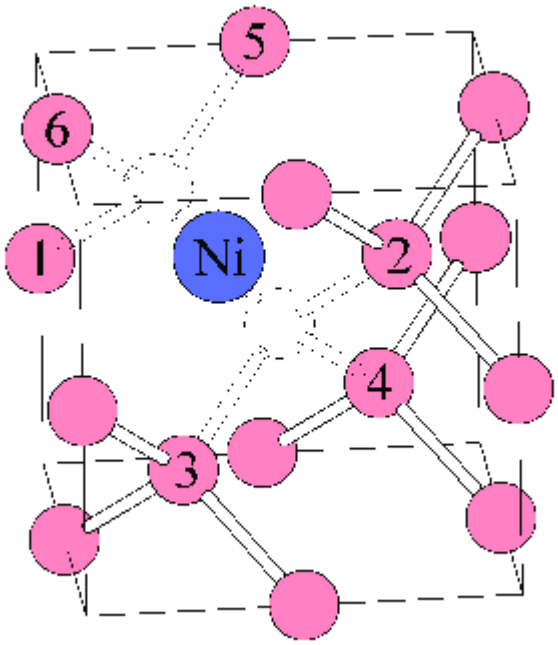

Figure 1.13 Nickel vacancy centers in diamond

Nickel centers, including the NE8, are other examples of sharp photo-luminescence peaks with small phonon coupling of the NV center, that has large phonon sidebands and ZPL of only around 4%. At room temperature, the NE8 center exhibits a ZPL at 802 nm with very small linewidths of 1–3 nm, and over 70% of the total emission is produced from this ZPL. Thanks to these properties, nickel-based centers could be more preferable to NV centers to produce on-demand identical single photons at room temperature, without the use of cryogenic cooling. Four nitrogen atoms enclose the nickel center to form the core of the NE8 center where it exists in structurally tetragonal-pyramidal geometry. In contrast to this, Ni-Si complexes form upon addition of nickel and silicon at the diamond core. This comes about during CVD or plasma assisted chemical vapor deposition. Depending on local charge state and stress, these complexes can emit narrow ZPLs at ≈767 nm and 865 nm. These Ni-related centers also tend to orient in certain <111> directions of the crystal, as do the Si-V centers. They also produce polarized light depending on their symmetry.

Syntheses and Spectral Properties

Doping of nickel-related centers can be carried out by at least two main ways: ion implantation and in situ doped CVD. In early work, Ni + ion dose was implanted with high energy and annealed at 800–1000°C to form the NE8 and its associated complexes. Nevertheless, the ion implantation method causes residual damage, and inhomogeneous distribution of defects.

More recently, the use of plasma enhanced chemical vapor deposition (PECVD) has taken over plasma-assisted CVD in the control addition of Ni and co-dopants such as silicon. Researchers have successfully found bright, spectrally stable Ni–Si centers by modifying precursor gas composition and substrate temperature in nanodiamond films [15]. The ideal doping conditions produce high concentration of optically active Ni–Si centers with low background fluorescence.

Quantum and Biomedical Technology Applications

Nickel- related color centers are particularly attractive for single-photon source applications owing to their high quantum efficiency, room-temperature operation as well as near line emission profiles. In photonic circuits, they provide a convenient way for optical waveguide coupling and are emitted in the NIR that coincides with the window of low-loss fiber transmission and have indispensable requirements for quantum communication [87].

In medical applications nickel-based nanodiamonds, Ni 0 and Ni–Si centers, are emerging as a new class of fluorescent labels. It has been reported that nanodiamonds below 100nm do not necessarily exhibit PL quenching as the size

Chapter 2. Experimental Equipment

For experiments used silicon wafer. First, wafer cut into small substrates with size 1x1cm2. Then for seeding ultrasonic bath (Elma S60H) was used. I used a MW CVD system SDS 6K (Seki Diamond, USA) similar to one which can be seen in figure 2.1. During experiment will use Torr units (USA standard, 1Torr = 133.322 Pa) instead of Si because CVD machine software uses USA unit.

1. Ultrasonic bath ((Elma S60H): The samples were prepared using an ultrasonic bath.
2. Microwave Plasma CVD reactor: An automated microwave plasma chemical reactor is used to synthesize diamond films and composites.

Figure 2.1 Microwave plasma CVD reactor

This sort of reactor is designed to produce a homogeneous flat plasma dispersion over the sample. The system consists of the following parts:

1. Vacuum chamber and vacuum system/pump.

2. Microwave radiation source.
3. A device for measuring the pressure and flow of gases
4. A device for measuring the temperature of sample.
5. Cooling system.
6. Stand for computer control:

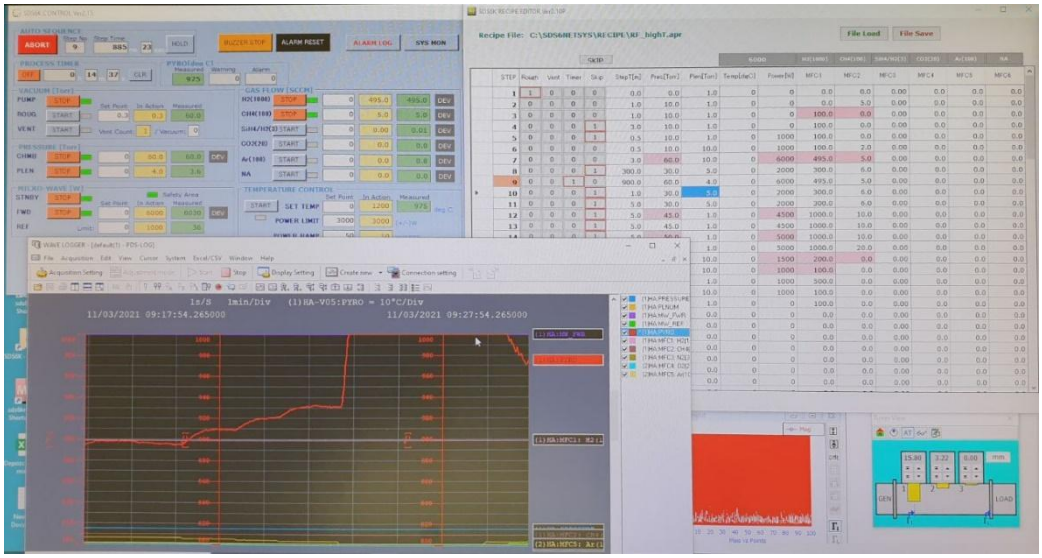

Figure 2.2 application to control the system

For evaluation we used scanning electron microscope (Mia 3, Tescan), In Via Reflex Raman spectrometer (Renishaw, similar to Figure 2.3) and optical microscope with spectrometer for thickness evaluation from interference fringes.

Figure 2.3 Raman spectrometer

Chapter 3. Results and discussion

Cleaning and pretreatment of substrates

First, polished Si substrates undergo cleaning. They are cleaned in three steps using acetone, followed by isopropyl alcohol and finally by deionized water. Each step was done in ultrasonic bath for 10 minutes.

Such a clean samples were seeded (pretreated) in a water solution of ultrafine detonation nanodiamond (510 nm grain size, NanoAmando, Japanin ultrasonic bath. Films were subjected to ultrasonic treatment for 10, 10, 20 minutes respectively to achieve a high nucleation density. Finally, samples were washed by deionized water and dried.

Synthesis of microcrystalline diamond films

Diamond films were deposited on pretreated silicon substrates with area 1x1cm^2 in CVD reactor in a mixture of gases CH_4/H_2. We selected two sets of experiments that differ by substrate temperature (T_S). We prepared a set of depositions to find out the deposition rate and film characteristics (morphology - SEM and quality - Raman) which will be used for later deposition Si-V containing diamond films. The CH_4/H_2 was kept constant 1 %. Total gas flow was also kept constant at 500 sccm together with the MW power delivered to the plasma which was 6 kW. The set of high T_S was prepared with the pressure in reactor 60 Torr, MW power of 6kW and plenum pressure of 7 Torr. The deposition time was 10, 30, 45, 60, 120, 240 min. The set of low T_S was prepared with the pressure in reactor 30 Torr, MW power of 6kW and plenum pressure of 4 Torr. Because the diamond deposition is temperature-controlled process, we increased the deposition times and experiments were done from 60 min to 24 hours.

Then a series of films was obtained. They differed in the concentration of SiH_4 and constant concentration of methane. The concentration of Si was calculated against C atom equal to 20, 100, 200, 400, 600 and were used for experiments. Scanning electron microscopy was used to evaluate the film surfaces and crystallite sizes (SEM). Then Raman and photoluminescence spectroscopy were performed at room temperature on a spectrometer.

Diamond morphology characteristics

For comparison, several samples were made with different deposit duration and deposition temperature. All films (Fig. 2.4.x and Fig. 2.5.x) consist of randomly oriented crystallites. Figures 2.4.x and 2.5.x shows SEM images of growth surfaces for films obtained at high resp. low substrate temperatures ($T_S \approx$ 950°C resp. $T_S \approx 450$°C)

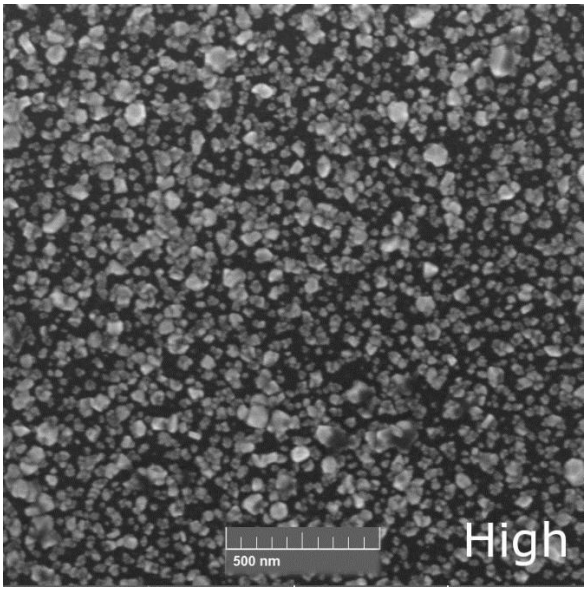

Figure 2.4.1 high deposition temperature – 10 min

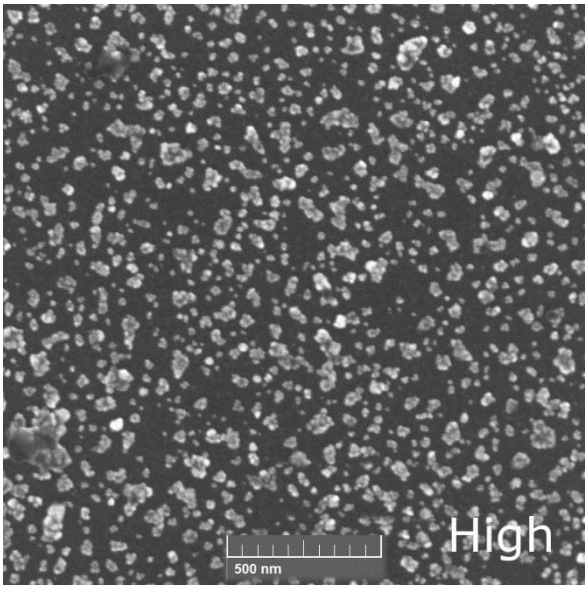

Figure 2.4.2 high deposition temperature – 20 min

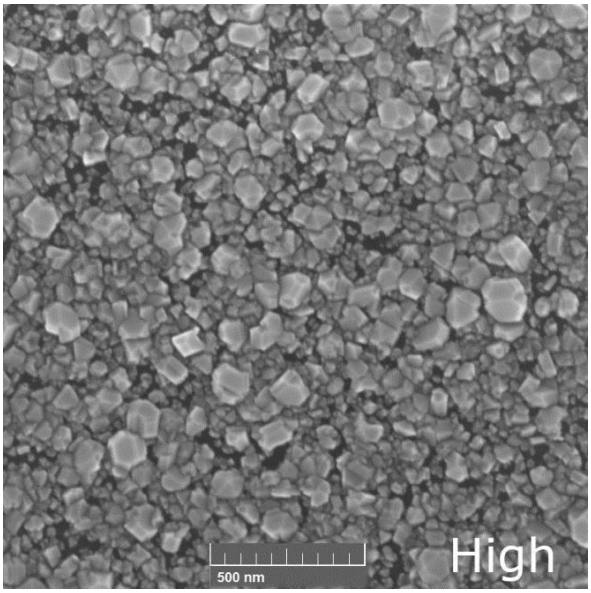

Figure 2.4.3 high deposition temperature - 30 min.

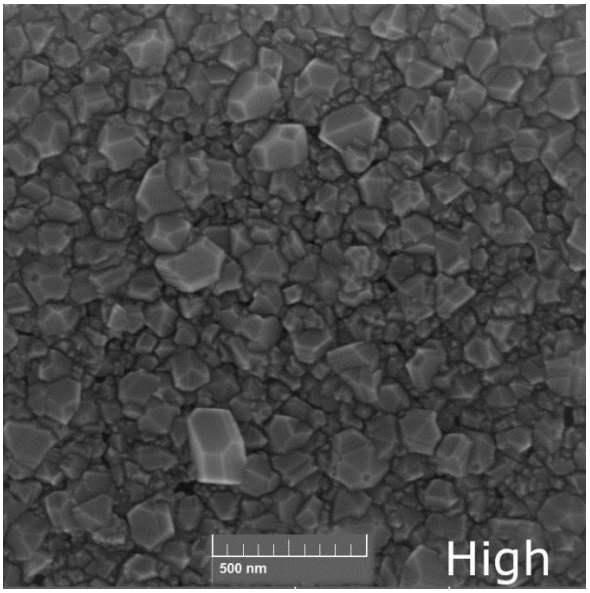

Figure 2.4.4 high deposition temperature- 45 min

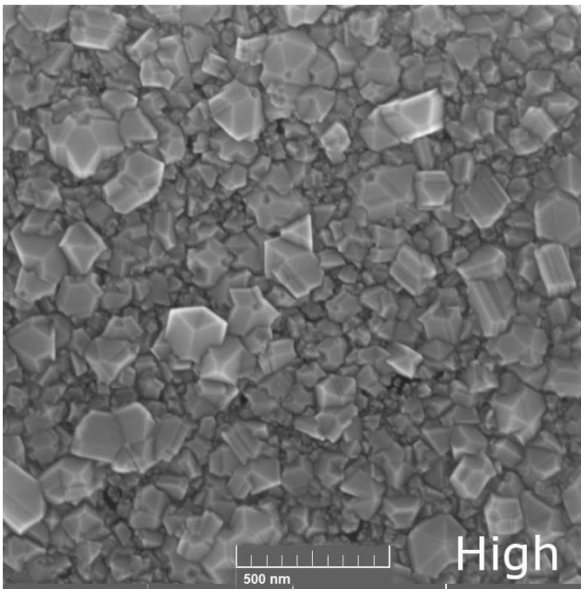

Figure 2.4.5 High deposition temperature - 1 hours

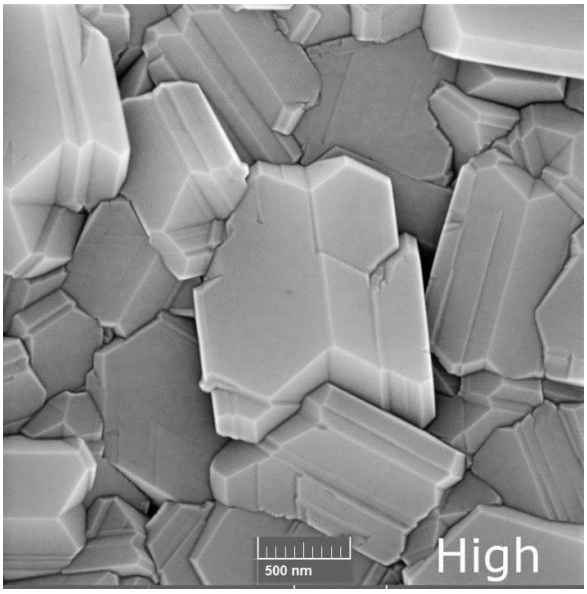

Figure 2.4.6 High deposition temperature - 4 hours

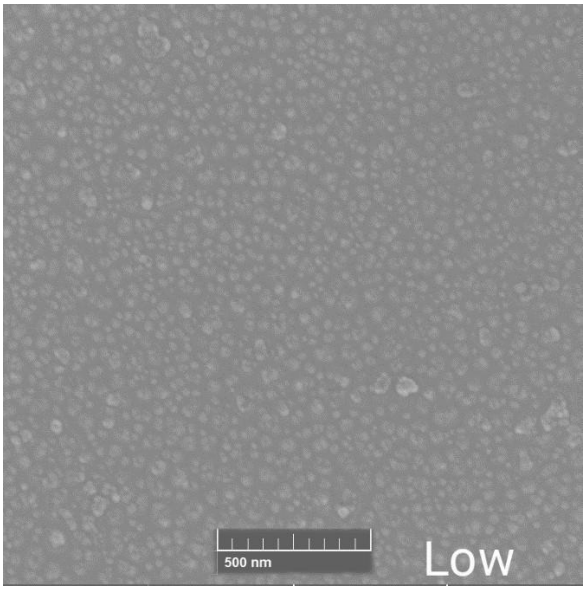

Figure 2.5.1 Low deposition temperature – 1 hours

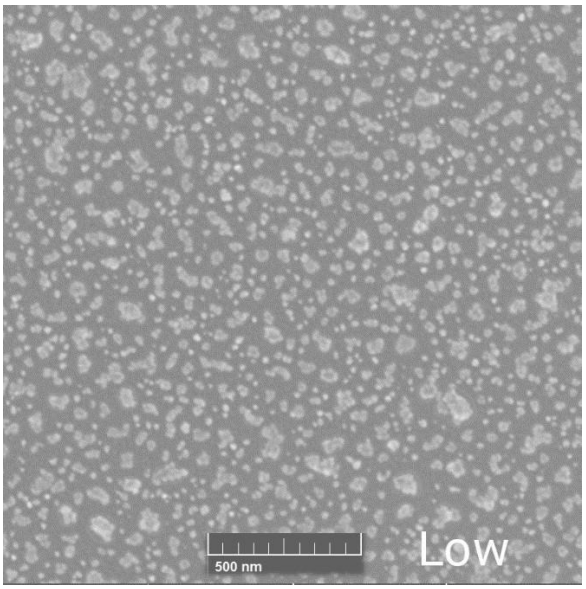

Figure 2.5.2 Low deposition temperature - 2 hours

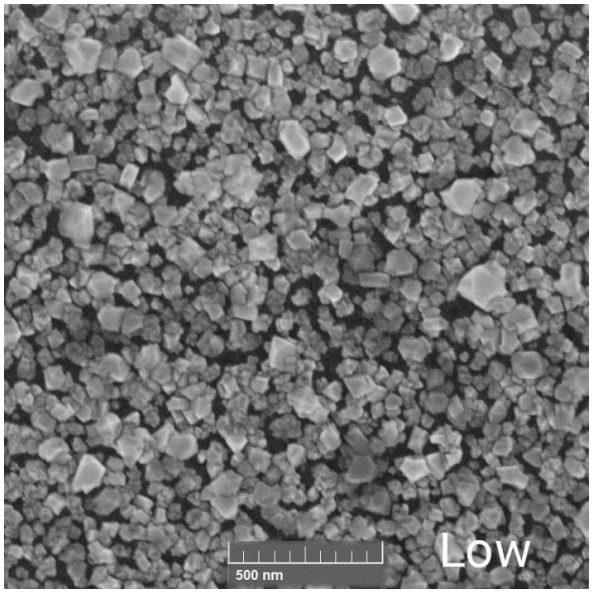

Figure 2.5.3 Low deposition temperature – 8 hours

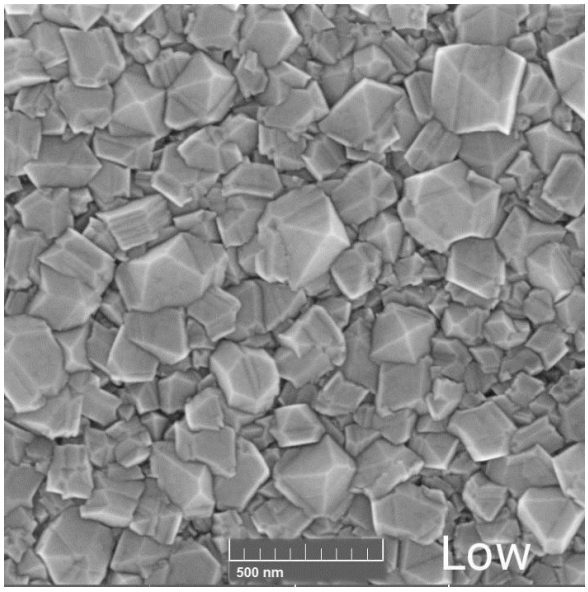

Figure 2.5.4 Low deposition temperature - 16 hours

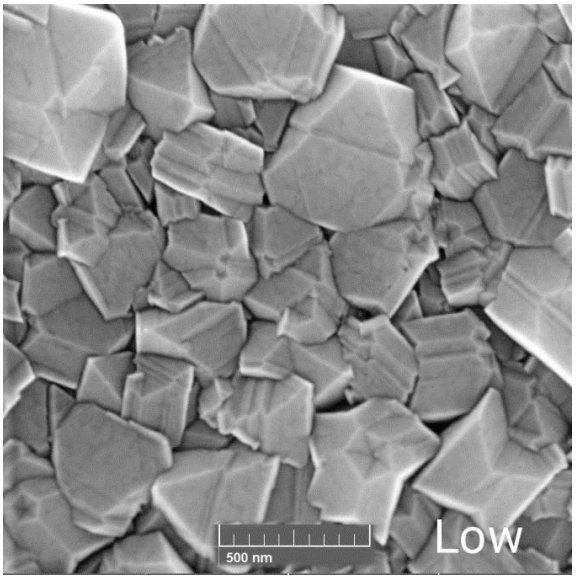

Figure 2.5.5 Low deposition temperature - 24 hours

At low temperatures and a short duration of deposition, the morphology of the surface remains unchanged, but at higher temperature, there is a tendency to reduce the grain size and the appearance of a larger number of twin defects. As we can see in Figure 2.5.x fully closing substrate for low Ts starting after 16 hours. For High Ts this process starts earlier because growth rate depends on deposition temperature

Thickness measurement and growth rate calculation

From the cross-section view (see typical result in Fig. 2.6.1 and Fig. 2.6.2) we analyzed the thickness of the films.

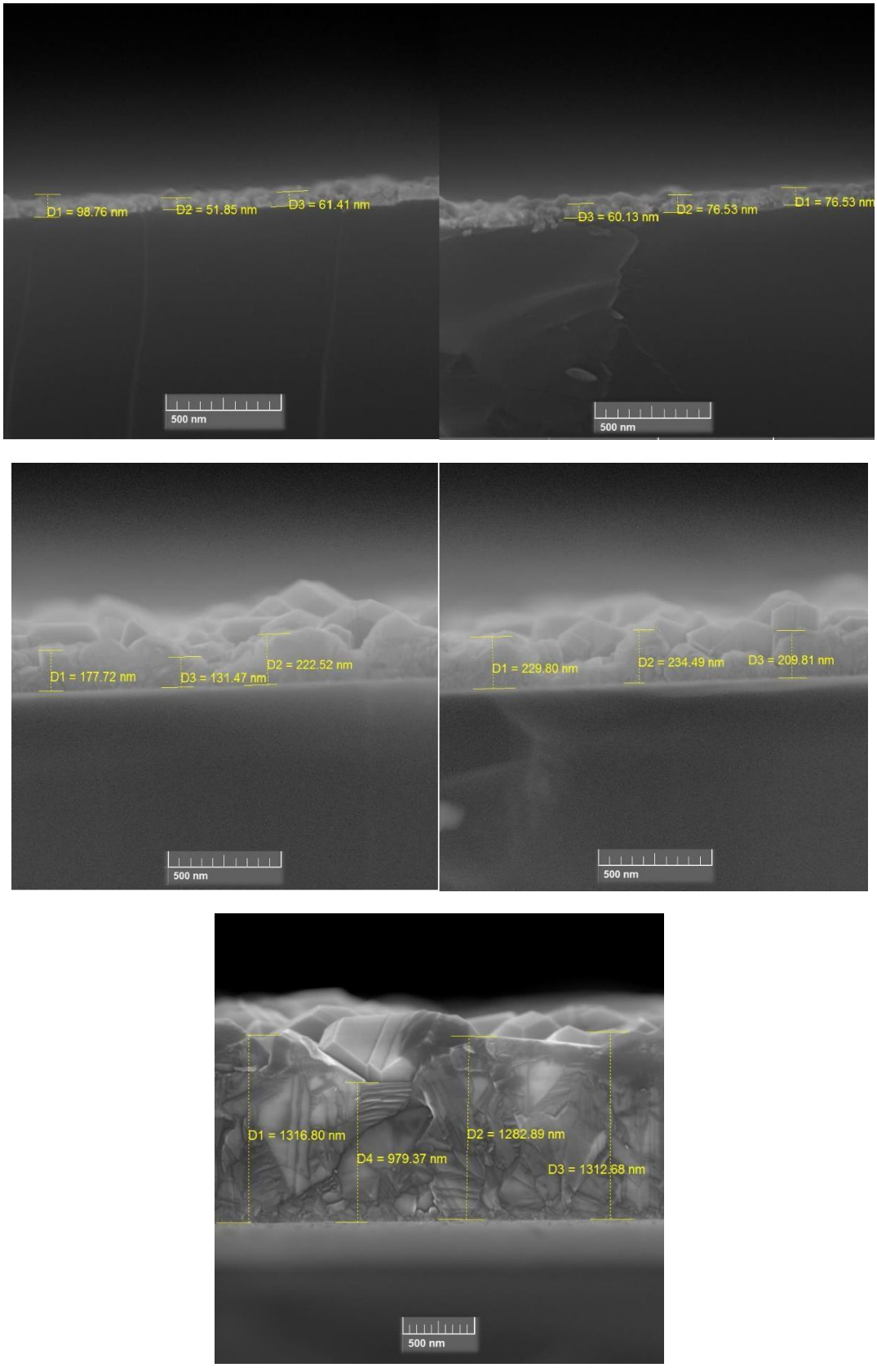

Figure 2.6.1 SEM cross section image with measurements for high TS

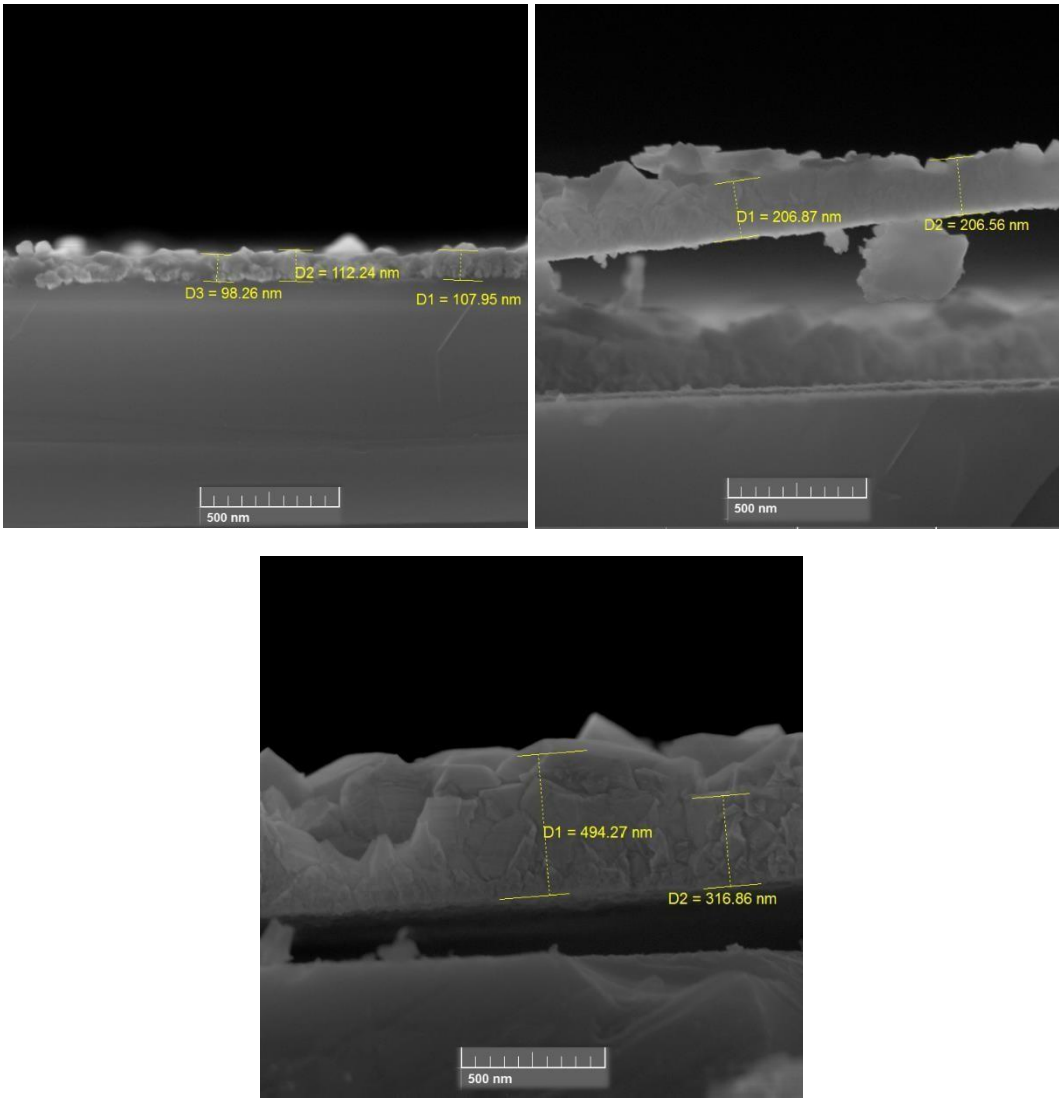

Figure 2.6.2 SEM cross section image with measurements for low TS

To determine the development of films thickness SEM in cross section were used (Tab. 1 and Tab 2.).

Measurment points	30 min		2h					4h			
	1	2	1	2	3	4	5	1	2	3	4
	nm	nm	nm	nm	nm	nm	nm	nm	nm	nm	nm
	98.76	60.13	143.19	177.72	229.80	154.7	272.25	1222.16	1316.80	1283.66	1362.57
	51.85	76.53	212.46	131.47	234.49	247.22	305.90	1130.0	1282.89	1166.84	1349.85
	61.41	76.53	299.59	222.52	209.81	367.90	226.61	1269.14	1312.68	1131.38	1246.97
						222.85	339.23		979.37		1259.96
Average:	70.67	71.06	218.41	177.24	224.70	248.1	286.0	1207.10	1222.94	1193.96	1304.84
Total Average	70.87		230.87					1232.21			
growth rate [nm/hour]:	141.74		115.44					308.05			

Table 1 SEM measurements for high temperature deposition

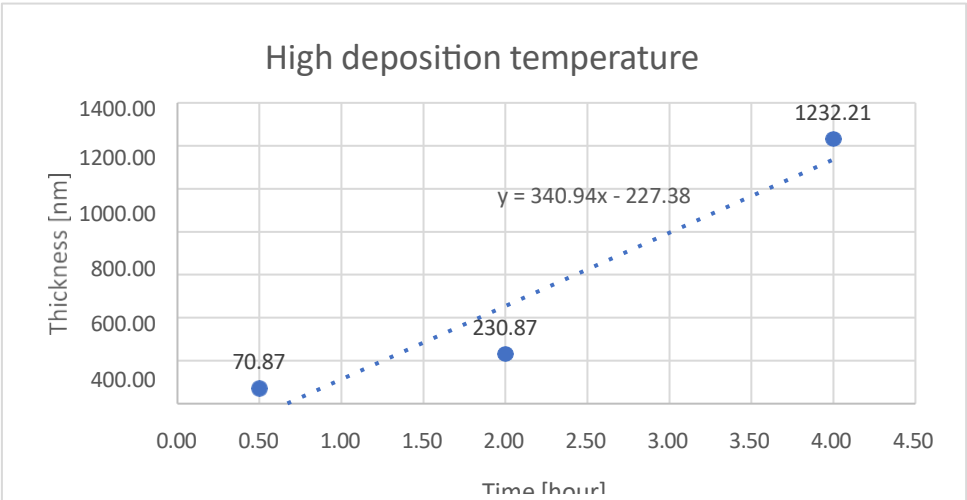

Figure 2.7 Dependence of the growth rate of diamond films on time for high deposition temperature with delay time 0.67 hours

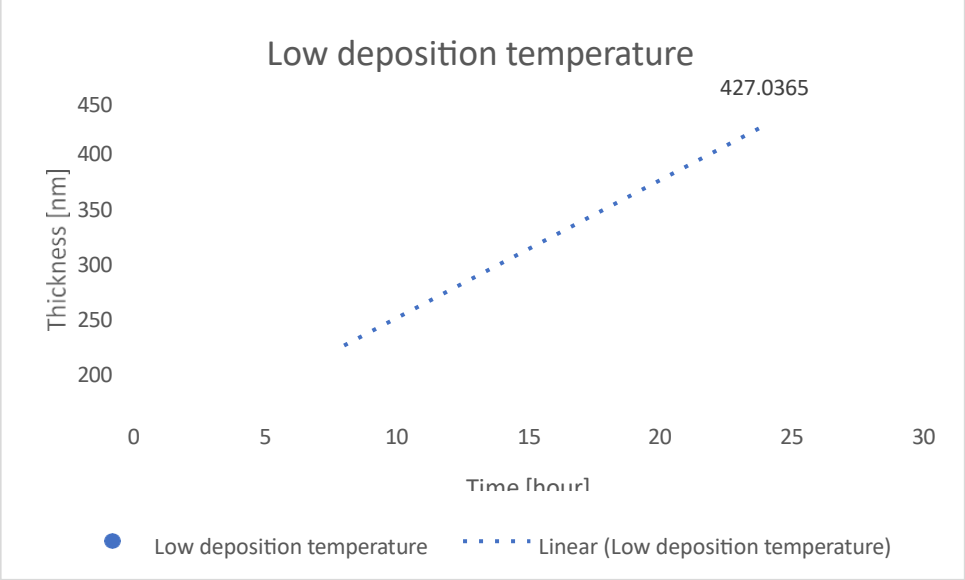

Figure 2.8 Dependence of the growth rate of diamond films on time for low deposition temperature with delay time 4.06 hours

	8h		16h				24h				
Measurment points	1	2	1	2	3	4	1	2	3	4	5
	nm	nm	nm	nm	nm	nm	nm	nm	nm	nm	nm
	98.26	108.57	212.08	206.87	253.64	219.46	494.27	456.60	466.55	404.82	469.91
	112.24	71.55	239.35	206.56	197.69	217.78	316.86	451.66	504.27	427.62	396.45
	107.95	84.86	160.83		237.76			385.02	423.45		
					219.14			508.13	325.19		
Average:	106.15	88.33	204.09	206.71	227.06	218.62	405.565	450.35	429.87	416.22	433.18
Total Average	97.24		214.12				427.04				
growth rate [nm/hour]:	12,25		13.38				17.79				

Table 2 SEM measurements for low temperature deposition

The growth rate of diamond films increases almost linearly from 12.15 to 17.79 for low and 35.43 to 308.05 microns / h for high deposition temperature. On a substrate with a low temperature, the growth rate of the sample is lower compared to high (Fig 2.7 and 2.8).

deposition time [min]	high Ts - deposition rate [nm/h]	low Ts - deposition rate [nm/h]
10	not possible to evaluate	not possible to evaluate
20	not possible to evaluate	not possible to evaluate
30	141,74	not possible to evaluate
45	not measured	not possible to evaluate
60	not measured	not possible to evaluate
120	115,44	not possible to evaluate
240	115,44	not possible to evaluate
480	308,05	12,25
960		13,38
1440		17,79

Table 3 Summary of calculated deposition rates for high and low deposition temperatures TS

At a substrate with low temperature, the growth rate of the sample from the high (Figure 2.9) is lower (17.5 nm / h) compared to the samples from the first batch (Figure 2.7) since the deposition temperatures are different.

Raman spectroscopy

Fig. 2.9 shows the Raman scattering spectra of films obtained at various deposition times and high and low deposition temperatures.

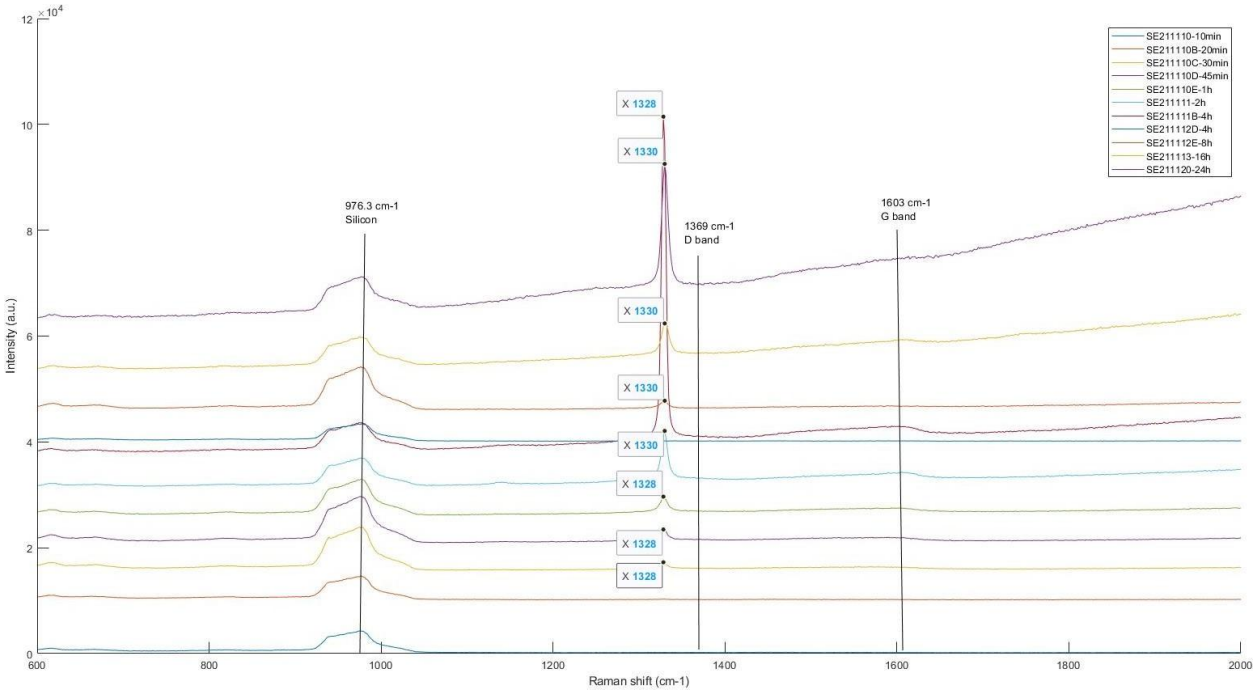

Figure 2.9 Raman scattering spectrum of a diamond film grown at low and high deposition temperatures

Where:

High Temp. Deposition samples	Low Temp. Deposition samples
SE211110	SE211112D
SE211110B	SE211112E
SE211110C	SE211113
SE211110D	
SE211110E	
SE211111	
SE211111B	

The G band is a result of in-plane vibrations of SP2 bonded carbon atoms.

The D band is vibrations associated with the breathing oscillation of full 6-membered carbon rings

PL

The photoluminescence spectra of films grown at a constant temperature and different SiH4 concentrations in the reactor are shown in Figure 2.10

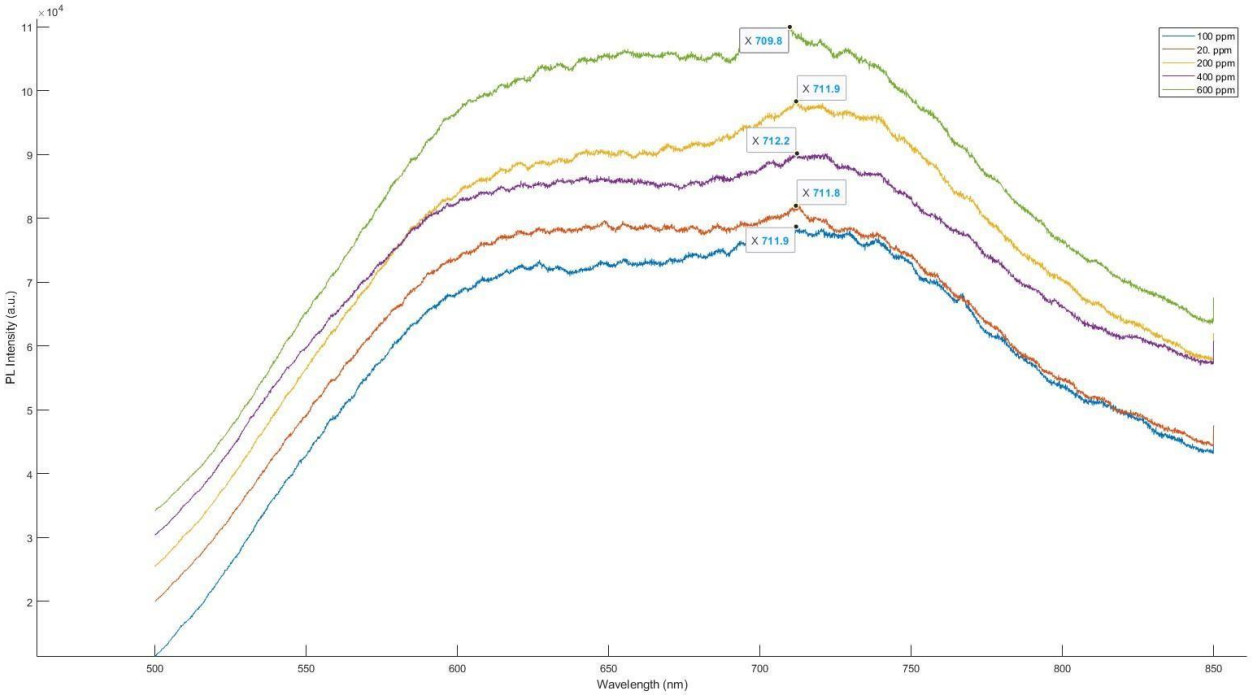

Figure 2.10 Photoluminescence spectra of microcrystalline diamond films grown at different SiH4 ratios

	SiH4	CH4	H2	Total	Wavelength
ppm	sccm				nm
20	0.1	5	494.9	500	711.8
100	0.5	5	494.5	500	711.9
200	1	5	494	500	711.7
400	2	5	493	500	712.2
600	4	5	491	500	709.8

Table 4 Concentration and Wavelength of PL of SiH4

The photoluminescence spectra shows a Si-V peak at a wavelength of 711.8 – 712.2 nm. The most interesting observation is the nonmonotonic dependence of the intensity of the Si-V peak on the Si/C ratio in the gas. PL increases at low concentrations of SiH4 (20ppm -2ppm%) and decreases with further addition of SiH_4 (Figure 2.10 and Table 4).

Conclusion

In the first part of the work, I reviewed the state of the fabrication and properties of diamond film and optical centers in diamond. The review includes various strategies for doping. Moreover, we extend the theoretical part by experimental activities where I succeeded with deposition of diamond films with optical centers. I did all the steps from the cleaning of the samples, their pretreatment by diamond seeds, and the chemical vapor deposition of diamond from the hydrogen/methane/silane gas mixture using commercial microwave plasma deposition system with specific software control.

In the first part we analyzed the correlation of selected process parameter, substrate temperature TS, with the diamond morphology and quality. I calculated the delay time and showed how the fully closed diamond film can be created and size of the grains controlled with respect to deposition time.

Based on these results I selected deposition condition for preparing diamond film with silicon vacancy optical centers by ingrowth during the deposition. I prepared two sets of samples for 60 minutes with various silane gas concentrations with the idea to influence the optical activity by surface termination. The photoluminescence data showed the optical center activity, but we did not observe very weak dependence on the surface termination. According to the literature further annealing can help with respect to formation of the silicon-vacancy centers and higher photoluminescence intensities and hence their changes.

Reference

1. Bennett C. H., Brassard G. Quantum cryptography: Public key distribution and coin tossing // International Conference on Computers, Systems & Signal Processing, Bangalore, India, Dec 912, 1984. 1984. P. 175–179.
2. Wootters W. K., Zurek W. H. A single quantum cannot be cloned // Nature. 1982. Vol. 299, no. 5886. P. 802–803.
3. Shalaev, V. M., Kinsey, N., Shaltout, A. M., Guler, U., Kim, J., Bogdanov, S., Shalaginov, M. Y., & Boltasseva, A. (2016). New material platforms and metasurface designs for nano- and quantum photonics (Conference Presentation). In G. S. Subramania & S. Foteinopoulou (Eds.), Active Photonic Materials VIII (p. 28). Active Photonic Materials VIII. SPIE.
4. Shalaginov, M. Y., Vorobyov, Vadim. V., Liu, J., Ferrera, M., Akimov, A. V., Lagutchev, A., Smolyaninov, Andrey. N., Klimov, V. V., Irudayaraj, J., Kildishev, A. V., Boltasseva, A., & Shalaev, V. M. (2014). Single-photon source based on NV center in nanodiamond coupled to TiN-based hyperbolic metamaterial. In CLEO: 2014 (p. JTu4A.38). CLEO: Applications and Technology. OSA.
5. Feynman, R. P. (1982). Simulating physics with computers. International Journal of Theoretical Physics, 21(6–7), 467–488.
6. Schaller, R. R. (1997). Moore’s law: past, present and future. IEEE Spectrum, 34(6), 52–59.
7. Shor, P. W. (1997). Polynomial-Time Algorithms for Prime Factorization and Discrete Logarithms on a Quantum Computer. SIAM Journal on Computing, 26(5), 1484–1509.

8. Monz, T., Schindler, P., Barreiro, J. T., Chwalla, M., Nigg, D., Coish, W. A., Harlander, M., Hänsel, W., Hennrich, M., & Blatt, R. (2011). 14-Qubit Entanglement: Creation and Coherence. Physical Review Letters, 106(13).
9. Wrachtrup, J., & Jelezko, F. (2006). Processing quantum information in diamond. Journal of Physics: Condensed Matter, 18(21), S807–S824
10. Barreiro, J. T., Müller, M., Schindler, P., Nigg, D., Monz, T., Chwalla, M., Hennrich, M., Roos, C. F., Zoller, P., & Blatt, R. (2011). An open-system quantum simulator with trapped ions. Nature, 470(7335), 486–491.
11. BUNDY, F. P., HALL, H. T., STRONG, H. M., & WENTORFJUN., R. H. (1955). Man-Made Diamonds. Nature, 176(4471), 51–55.
12. Vlasov, I. I., Barnard, A. S., Ralchenko, V. G., Lebedev, O. I., Kanzyuba, M. V., Saveliev, A. V., Konov, V. I., & Goovaerts, E. (2009). Nanodiamond Photoemitters Based on Strong Narrow-Band Luminescence from Silicon-Vacancy Defects. Advanced Materials, 21(7), 808–812.
13. Pezzagna, S., Rogalla, D., Wildanger, D., Meijer, J., & Zaitsev, A. (2011). Creation and nature of optical centres in diamond for single-photon emission—overview and critical remarks. New Journal of Physics, 13(3), 035024.
14. Rabeau, J. R., Chin, Y. L., Prawer, S., Jelezko, F., Gaebel, T., & Wrachtrup, J. (2005). Fabrication of single nickel-nitrogen defects in diamond by chemical vapor deposition. Applied Physics Letters, 86(13).
15. Steinmetz, D., Neu, E., Meijer, J., Bolse, W., & Becher, C. (2011). Single photon emitters based on Ni/Si related defects in single crystalline diamond. Applied Physics B, 102(3), 451–458.
16. Magyar, A., Hu, W., Shanley, T., Flatté, M. E., Hu, E., & Aharonovich, I. (2014). Synthesis of luminescent europium defects in diamond. Nature Communications, 5(1).
17. RAMAN, C. V. (1943). THE STRUCTURE AND PROPERTIES OF DIAMOND. *Current Science*, *12*(1), 33–42.
18. Nikerov, M. V., Bochvar, D. A., & Stankevich, I. V. (1982). Allotropic modifications of carbon. Journal of Structural Chemistry, 23(1), 150–152.
19. Almeida, F. A., Amaral, M., Oliveira, F. J., & Silva, R. F. (2006). Machining behaviour of silicon nitride tools coated with micro-, submicro- and nanometric HFCVD diamond crystallite sizes. Diamond and Related Materials, 15(11–12), 2029–2034.
20. Polini, R., Barletta, M., & Cristofanilli, G. (2010). Wear resistance of nano- and micro-crystalline diamond coatings onto WC–Co with Cr/CrN interlayers. Thin Solid Films, 519(5), 1629–1635
21. Raghuveer, M. S., Yoganand, S. N., Jagannadham, K., Lemaster, R. L., & Bailey, J. (2002). Improved CVD diamond coatings on WC–Co tool substrates. Wear, 253(11–12), 1194–1206
22. Deuerler, F., Gruner, H., Pohl, M., & Tikana, L. (2001). Wear mechanisms of diamond-coated tools. Surface and Coatings Technology, 142–144, 674–680.
23. Aharonovich, I., & Prawer, S. (2010). Fabrication strategies for diamond based ultra bright single photon sources. Diamond and Related Materials, 19(7–9), 729–733.
24. Neu, E., Arend, C., Gross, E., Guldner, F., Hepp, C., Steinmetz, D., Zscherpel, E., Ghodbane, S., Sternschulte, H., Steinmüller-Nethl, D., Liang, Y., Krueger, A., & Becher, C. (2011). Narrowband fluorescent nanodiamonds produced from chemical vapor deposition films. Applied Physics Letters, 98(24).
25. Riedrich-Möller, J., Kipfstuhl, L., Hepp, C. *et al.* One- and two-dimensional photonic crystal microcavities in single crystal diamond. *Nature Nanotech* **7**, 69–74 (2012).
26. Weijer, C. J. (2003). Visualizing Signals Moving in Cells. Science, 300(5616), 96–100.

27. Hardman, R. (2006). A Toxicologic Review of Quantum Dots: Toxicity Depends on Physicochemical and Environmental Factors. Environmental Health Perspectives, 114(2), 165–172.
28. Yu, S.-J., Kang, M.-W., Chang, H.-C., Chen, K.-M., & Yu, Y.-C. (2005). Bright Fluorescent Nanodiamonds: No Photobleaching and Low Cytotoxicity. Journal of the American Chemical Society, 127(50), 17604–17605.
29. Lam, R., & Ho, D. (2009). Nanodiamonds as vehicles for systemic and localized drug delivery. Expert Opinion on Drug Delivery, 6(9), 883–895.
30. Chang, H.-C. (2009). Development and Use of Fluorescent Nanodiamonds as Cellular Markers. In Nanodiamonds (pp. 127–150). Springer US.
31. Han, K. Y., Willig, K. I., Rittweger, E., Jelezko, F., Eggeling, C., & Hell, S. W. (2009). Three-Dimensional Stimulated Emission Depletion Microscopy of Nitrogen-Vacancy Centers in Diamond Using Continuous-Wave Light. Nano Letters, 9(9), 3323–3329.
32. Taylor, A.C., González, C.H., Miller, B. *et al.* Surface functionalisation of nanodiamonds for human neural stem cell adhesion and proliferation. *Sci Rep* **7**, 7307 (2017).
33. Vlasov, I., Shiryaev, A., Rendler, T. *et al.* Molecular-sized fluorescent nanodiamonds. *Nature Nanotech* **9**, 54–58 (2014).
34. Neu, E., Steinmetz, D., Riedrich-Möller, J., Gsell, S., Fischer, M., Schreck, M., & Becher, C. (2011). Single photon emission from silicon-vacancy colour centres in chemical vapour deposition nano-diamonds on iridium. New Journal of Physics, 13(2), 025012.
35. Sapozhnikov, M. N. (1978). Properties of the zero-phonon lines in the optical spectra of molecular crystals. The Journal of Chemical Physics, 68(5), 2352–2361.
36. Jelezko, F., & Wrachtrup, J. (2006). Single defect centres in diamond: A review. Physica Status Solidi (a), 203(13), 3207–3225.
37. Rabeau, J. R., Stacey, A., Rabeau, A., Prawer, S., Jelezko, F., Mirza, I., & Wrachtrup, J. (2007). Single Nitrogen Vacancy Centers in Chemical Vapor Deposited Diamond Nanocrystals. Nano Letters, 7(11), 3433–3437.
38. Gaebel, T., Popa, I., Gruber, A., Domhan, M., Jelezko, F., & Wrachtrup, J. (2004). Stable single-photon source in the near infrared. New Journal of Physics, 6, 98–98.
39. Czelej, K., Ćwieka, K., Śpiewak, P., & Jan Kurzydłowski, K. (2018). Titanium-related color centers in diamond: a density functional theory prediction. Journal of Materials Chemistry C, 6(19), 5261–5268.
40. Sandstrom, R., Ke, L., Martin, A., Wang, Z., Kianinia, M., Green, B., Gao, W., & Aharonovich, I. (2018). Optical properties of implanted Xe color centers in diamond. Optics Communications, 411, 182–186.
41. Page, T. F. (1991). Ion Implantation. In Concise Encyclopedia of Advanced Ceramic Materials (pp. 252–257). Elsevier.
42. Auberton-Herve, A., Wittkower, A., & Aspar, B. (1995). SIMOX — a new challenge for ion implantation. Nuclear Instruments and Methods in Physics Research Section B: Beam Interactions with Materials and Atoms, 96(1–2), 420–424.
43. Wolverson, D. (2008). Raman spectroscopy. In Characterization of Semiconductor Heterostructures and Nanostructures (pp. 249–288). Elsevier.
44. Palyanov, Y. N., Kupriyanov, I. N., Khokhryakov, A. F., & Ralchenko, V. G. (2015). Crystal Growth of Diamond. In Handbook of Crystal Growth (pp. 671–713). Elsevier.

45. Khachatryan, A. Kh., Aloyan, S. G., May, P. W., Sargsyan, R., Khachatryan, V. A., & Baghdasaryan, V. S. (2008). Graphite-to-diamond transformation induced by ultrasound cavitation. Diamond and Related Materials, 17(6), 931–936.
46. Ando, Y., Tobe, S., Saito, T., Sakurai, J., Tahara, H., & Yoshikawa, T. (2004). Enlargement of the diamond deposition area in combustion flame method by traversing substrate. Thin Solid Films, 457(1), 217–223.
47. Smolin, A. A., Ralchenko, V. G., Pimenov, S. M., Kononenko, T. V., & Loubnin, E. N. (1993). Optical monitoring of nucleation and growth of diamond films. Applied Physics Letters, 62(26), 3449–3451.
48. Das, D., & Singh, R. N. (2007). A review of nucleation, growth and low temperature synthesis of diamond thin films. International Materials Reviews, 52(1), 29–64.
49. Ralchenko, V., Pimenov, S., Konov, V., Khomich, A., Saveliev, A., Popovich, A., Vlasov, I., Zavedeev, E., Bozhko, A., Loubnin, E., & Khmelnitskii, R. (2007). Nitrogenated nanocrystalline diamond films: Thermal and optical properties. Diamond and Related Materials, 16(12), 2067–2073.
50. Widmann, C. J., Hetzl, M., Drieschner, S., & Nebel, C. E. (2017). Homoepitaxial growth of high quality (111)-oriented single crystalline diamond. Diamond and Related Materials, 72, 41–46.
51. Bushuev, E. V., Yurov, V. Yu., Bolshakov, A. P., Ralchenko, V. G., Khomich, A. A., Antonova, I. A., Ashkinazi, E. E., Shershulin, V. A., Pashinin, V. P., & Konov, V. I. (2017). Express in situ measurement of epitaxial CVD diamond film growth kinetics. Diamond and Related Materials, 72, 61–70.
52. Bachmann, P. K., Leers, D., & Lydtin, H. (1991). Towards a general concept of diamond chemical vapour deposition. Diamond and Related Materials, 1(1), 1–12.
53. Prijaya, N. A., Angus, J. C., & Bachmann, P. K. (1994). Thermochemical computation of the diamond deposition domain. Diamond and Related Materials, 3(1–2), 129–136.
54. Strong, H. M., & Chrenko, R. M. (1971). Diamond growth rates and physical properties of laboratory-made diamond. The Journal of Physical Chemistry, 75(12), 1838–1843.
55. Tendero, C., Tixier, C., Tristant, P., Desmaison, J., & Leprince, P. (2006). Atmospheric pressure plasmas: A review. Spectrochimica Acta Part B: Atomic Spectroscopy, 61(1), 2–30.
56. May, P. W., Smith, J. A., & Mankelevich, Y. A. (2006). Deposition of NCD films using hot filament CVD and Ar/CH4/H2 gas mixtures. *Diamond and Related Materials*, *15*(2-3), 345–352.
57. Fuentes-Fernandez, E. M. A., Alcantar-Peña, J. J., Lee, G., Boulom, A., Phan, H., Smith, B., … Auciello, O. (2016). Synthesis and characterization of microcrystalline diamond to ultrananocrystalline diamond films via Hot Filament Chemical Vapor Deposition for scaling to large area applications. *Thin Solid Films*, *603*, 62–68.
58. Schwander, M., & Partes, K. (2011). A review of diamond synthesis by CVD processes. *Diamond and Related Materials*, *20*(9), 1287–1301.
59. L. Regel, L., & R. Wilcox, W. (2001). Diamond film deposition by chemical vapor transport. *Acta Astronautica*, *48*(2-3), 129–144.
60. Matsui, Y., Yabe, H., & Hirose, Y. (1990). The Growth Mechanism of Diamond Crystals in Acetylene Flames. Japanese Journal of Applied Physics, 29(Part 1, No. 8), 1552–1560.
61. Murayama, M., Kojima, S., & Uchida, K. (1991). Uniform deposition of diamond films using a flat flame stabilized in the stagnation-point flow. *Journal of Applied Physics*, *69*(11), 7924–7926.

62. Donnet, J. B., Oulanti, H., Huu, T. L., & Schmitt, M. (2006). Synthesis of large single crystal diamond using combustion-flame method. *Carbon*, *44*(2), 374–380.
63. Schmitt, M., & Paulmier, D. (2004). Tribological behaviour of diamond coatings sliding against Al alloys. *Tribology International*, *37*(4), 317–325.
64. Kurihara, K., Sasaki, K., Kawarada, M., & Koshino, N. (1988). High rate synthesis of diamond by dc plasma jet chemical vapor deposition. *Applied Physics Letters*, *52*(6), 437–438.
65. Berthou, H., Faure, C., Hänni, W., & Perret, A. (1999). Morphology and Raman spectra of diamond films grown with a plasma torch. *Diamond and Related Materials*, *8*(2-5), 636–639.
66. Silva, F., Hassouni, K., Bonnin, X., & Gicquel, A. (2009). Microwave engineering of plasmaassisted CVD reactors for diamond deposition. *Journal of Physics: Condensed Matter*, *21*(36), 364202.
67. Donnelly, K., Dowling, D. P., McConnell, M. L., Flood, R. V., Berkefelt, O., & Svennebrink, J. (2000). Diamond deposition using a novel microwave applicator. Diamond and Related Materials, 9(3-6), 693–697.
68. Vollertsen, F., Partes, K., & Schubnov, A. (2009). Thin nanocrystalline diamond films deposited by LaPlas-CVD at atmospheric pressure. *Production Engineering*, *4*(1), 9–14.
69. Mistry, P., Turchan, M. C., Granse, G. O., & Baurmann, T. (1997). New rapid diamond synthesis technique; using multiplexed pulsed lasers in laboratory ambients. Materials Research Innovations, 1(3), 149–156.
70. Rosenkranz, B. (2000). Microwave-induced plasma–optical emission spectrometry – fundamental aspects and applications in metal speciation analysis. TrAC Trends in Analytical Chemistry, 19(23), 138–156.
71. Morgan, C. G. (1975). Laser-induced breakdown of gases. Reports on Progress in Physics, 38(5), 621–665.
72. Seely, J. F., & Harris, E. G. (1973). Heating of a Plasma by Multiphoton Inverse Bremsstrahlung. Physical Review A, 7(3), 1064–1067.
73. Metev, S., Stephen, A., Schwarz, J., & Wochnowski, C. (2004). Laser-induced chemistry: an advanced tool for micro structuring, synthesis, and modification of materials.
74. Sapozhnikov, M. N. (1978, March 1). Properties of the Zero-phonon lines in the optical spectra of molecular crystals. AIP Publishing. Retrieved January 4, 2022
75. Chen, YC., Salter, P., Knauer, S. et al. Laser writing of coherent colour centres in diamond. Nature Photon 11, 77–80 (2017).
76. Collins, A., Kamo, M., & Sato, Y. (1990). A spectroscopic study of optical centers in diamond grown by microwave-assisted chemical vapor deposition. Journal of Materials Research, 5(11), 2507-2514.
77. Hui, Y. Y., Cheng, C.-L., & Chang, H.-C. (2010). Nanodiamonds for optical bioimaging. Journal of Physics D: Applied Physics, 43(37), 374021.
78. Castelletto, S., & Edmonds, A. (2012). 680-890nm spectral range of nickel-nitrogen and nickelsilicon complex single centres in diamond. Quantum Communications and Quantum Imaging X.
79. Zaitsev, A. M. (2000). Vibronic spectra of impurity-related optical centers in diamond. Physical Review B, 61(19), 12909–12922.
80. Neu, E., & Aharonovich, I. (2014). Diamond Nanophotonics. Advanced Optical Materials, 2(10), 911–928.

81. Burns, R. C., Cvetkovic, V., Dodge, C. N., Evans, D. J. F., Rooney, M.-L. T., Spear, P. M., & Welbourn, C. M. (1990). Growth-sector dependence of optical features in large synthetic diamonds. Journal of Crystal Growth, 104(2), 257–279.
82. Rogers, L. J., Jahnke, K. D., Doherty, M. W., Dietrich, A., McGuinness, L. P., Müller, C., … Jelezko, F. (2014). Electronic structure of the negatively charged silicon-vacancy center in diamond. Physical Review B, 89(23).
83. Sohn, YI., Meesala, S., Pingault, B. et al. Controlling the coherence of a diamond spin qubit through its strain environment. Nat Commun 9, 2012 (2018).
84. Balmer, R. S., Brandon, J. R., Clewes, S. L., Dhillon, H. K., Dodson, J. M., Friel, I., … Woollard, S. M. (2009). Chemical vapour deposition synthetic diamond: materials, technology and applications. Journal of Physics: Condensed Matter, 21(36), 364221.
85. CUI, Y.-xiao, ZHANG, J.-guo, SUN, F.-hong, & ZHANG, Z.-ming. (2013). Si-doped diamond films prepared by chemical vapour deposition. Transactions of Nonferrous Metals Society of China, 23(10), 2962–2970.
86. Silva, F. J. G., Fernandes, A. J. S., Costa, F. M., Teixeira, V., Baptista, A. P. M., & Pereira, E. (2003). Tribological behaviour of CVD diamond films on steel substrates. Wear, 255(7-12), 846–853.
87. Aharonovich, I., Zhou, C., Stacey, A., Orwa, J., Castelletto, S., Simpson, D., Greentree, A. D., Treussart, F., Roch, J.-F., & Prawer, S. (2009). Enhanced single-photon emission in the near infrared from a diamond color center. Physical Review B, 79(23).